



ΕΘΝΙΚΟ ΜΕΤΣΟΒΙΟ ΠΟΛΥΤΕΧΝΕΙΟ
ΣΧΟΛΗ ΗΛΕΚΤΡΟΛΟΓΩΝ ΜΗΧΑΝΙΚΩΝ ΚΑΙ ΜΗΧΑΝΙΚΩΝ ΥΠΟΛΟΓΙΣΤΩΝ
ΤΟΜΕΑΣ ΜΗΧΑΝΟΛΟΓΙΚΩΝ ΚΑΤΑΣΚΕΥΩΝ & ΑΥΤΟΜΑΤΟΥ ΕΛΕΓΧΟΥ

Χειρισμός αντικειμένου
από ρομποτικούς βραχίονες
μεταφερόμενης βάσης με
αποκεντρωμένο έλεγχο έμμεσης
επικοινωνίας

ΔΙΠΛΩΜΑΤΙΚΗ ΕΡΓΑΣΙΑ

του

Τσιάμη Ε. Αναστάσιου

Επιβλέπων : Κωνσταντίνος Ι. Κυριακόπουλος
Καθηγητής Ε.Μ.Π.

ΕΡΓΑΣΤΗΡΙΟ ΑΥΤΟΜΑΤΟΥ ΕΛΕΓΧΟΥ
Αθήνα, Σεπτέμβριος 2014



Εθνικό Μετσόβιο Πολυτεχνείο
Σχολή Ηλεκτρολόγων Μηχανικών και Μηχανικών Υπολογιστών
Τομέας Μηχανολογικών Κατασκευών & Αυτομάτου Ελέγχου
Εργαστήριο Αυτομάτου Ελέγχου

Χειρισμός αντικειμένου
από ρομποτικούς βραχίονες
μεταφερόμενης βάσης με
αποκεντρωμένο έλεγχο έμμεσης
επικοινωνίας

ΔΙΠΛΩΜΑΤΙΚΗ ΕΡΓΑΣΙΑ

του

Τσιάμη Ε. Αναστάσιου

Επιβλέπων : Κωνσταντίνος Ι. Κυριακόπουλος
Καθηγητής Ε.Μ.Π.

Εγκρίθηκε από την τριμελή εξεταστική επιτροπή την 1η Σεπτεμβρίου 2014.

.....
Κων/νος Κυριακόπουλος Νικόλαος Μαράτος
Καθηγητής Ε.Μ.Π. Καθηγητής Ε.Μ.Π.

.....
Κων/νος Τζαφέστας
Επ. Καθηγητής Ε.Μ.Π.

Αθήνα, Ιούλιος 2014

.....
ΤΣΙΑΜΗΣ ΑΝΑΣΤΑΣΙΟΣ
Διπλωματούχος Ηλεκτρολόγος Μηχανικός και Μηχανικός Υπολογιστών
Ε.Μ.Π.

Copyright © Τσιάμης Αναστάσιος, 2014.
Με επιφύλαξη παντός δικαιώματος. All rights reserved.

Απαγορεύεται η αντιγραφή, αποθήκευση και διανομή της παρούσας εργασίας, εξ ολοκλήρου ή τμήματος αυτής, για εμπορικό σκοπό. Επιτρέπεται η ανατύπωση, αποθήκευση και διανομή για σκοπό μη κερδοσκοπικό, εκπαιδευτικής ή ερευνητικής φύσης, υπό την προϋπόθεση να αναφέρεται η πηγή προέλευσης και να διατηρείται το παρόν μήνυμα. Ερωτήματα που αφορούν τη χρήση της εργασίας για κερδοσκοπικό σκοπό πρέπει να απευθύνονται προς τον συγγραφέα.

Οι απόψεις και τα συμπεράσματα που περιέχονται σε αυτό το έγγραφο εκφράζουν τον συγγραφέα και δεν πρέπει να ερμηνευθεί ότι αντιπροσωπεύουν τις επίσημες θέσεις του Εθνικού Μετσόβιου Πολυτεχνείου.

Ευχαριστίες

Ευχαριστώ θερμά τον καθηγητή Κ. Κυριακόπουλο για την ανάθεση αυτής της διπλωματικής εργασίας και για την ευκαιρία που μου έδωσε να συμμετέχω στην έρευνα του εργαστηρίου Αυτομάτου Ελέγχου. Ιδιαίτερα ευχαριστώ τον επιστημονικό συνεργάτη δρ. Μπάμπη Μπεχλιούλη για την πολύτιμη βοήθεια που μου παρείχε και για τον εμπλουτισμό των γνώσεών μου στην περιοχή των μη-γραμμικών συστημάτων. Ακόμη, θέλω να ευχαριστήσω θερμά τους γονείς μου για την στήριξη που μου παρείχαν κατά τη διάρκεια των σπουδών μου και την αδερφή μου, για τις πολύτιμες συμβουλές της. Τέλος, πολύ θερμά ευχαριστώ στην Καλλιόπη και όλους τους φίλους μου, που μου στάθηκαν τα τελευταία χρόνια.

Περίληψη

Με την αύξηση του αριθμού των ρομποτικών πρακτόρων που απαιτούνται για την αποκεντρωμένη ολοκλήρωση μιας εργασίας, αλλά και λόγω του απαιτητικού περιβάλλοντος εκτέλεσης, γίνονται προσπάθειες να περιοριστεί η ποσότητα της άμεσης πληροφορίας που ανταλλάσσεται μεταξύ τους. Μία πιθανή λύση είναι η αξιοποίηση της έμμεσης πληροφορίας, που προκύπτει από την αλληλεπίδραση του ρομπότ με το περιβάλλον και λαμβάνεται από τις μετρήσεις των αισθητήρων. Αυτός ο τρόπος επικοινωνίας ονομάζεται έμμεση επικοινωνία.

Το αντικείμενο αυτής της διπλωματικής, είναι η ενσωμάτωση αυτού του σχήματος επικοινωνίας στο χειρισμό αντικειμένου από δύο ρομποτικούς πράκτορες. Η διάταξη είναι τύπου αρχηγού-ακολούθου και αποκεντρωμένη. ο αρχηγός προσπαθεί να υλοποιήσει επιθυμητή τροχιά, ενώ ο ακόλουθος χρησιμοποιεί μόνο μέτρηση δύναμης, θέσης και ταχύτητας, για να βοηθήσει την εκτέλεση της εργασίας. Εξετάζονται δύο σενάρια με διαφορετικές υλοποιήσεις.

Στο πρώτο, το αντικείμενο είναι σχήματος ράβδου και μεταφέρεται από έντροχα μη ολονομικά ρομποτ, με ελαστική-συμμορφούμενη επαφή του ακολούθου με το αντικείμενο. Ο ακόλουθος χρησιμοποιεί μέτρηση δύναμης-ροπής για να ευθυγραμμιστεί με το αντικείμενο και να διατηρήσει την επαφή. Το συνολικό σύστημα συμπεριφέρεται σαν ένα διαταραγμένο μοντέλο αυτοκινήτου, οπότε ο αρχηγός βασιζόμενος σε μια ανάλυση ευρωστίας, χρησιμοποιεί ελεγχτή που εφαρμόζεται στο ονομαστικό μοντέλο.

Στο δεύτερο, το αντικείμενο μεταφέρεται από έντροχους βραχίονες και οι επαφές είναι στερεές. Και τα δύο ρομπότ επιβάλλουν σε αυτό μια σχέση ελέγχου εμπέδησης. Ο ακόλουθος, μέσα από την κίνηση του αντικειμένου, εκτιμά το προφίλ τροχιάς του αρχηγού με εύρωστο τρόπο. Τελικά, το σφάλμα τροχιάς του αντικειμένου συγκλίνει σε μία πολύ μικρή περιοχή γύρω από το μηδέν.

Λέξεις Κλειδιά

Αποκεντρωμένος Έλεγχος, Έμμεση Επικοινωνία, Μεταφορά Αντικειμένου, Μέτρηση Δύναμης, Αρχηγός- Ακόλουθος, Μη Ολονομικό Σύστημα

Abstract

Facing the increasing number of robotic agents required in distributed coordinated tasks and due to challenging environment of execution, attempts are made to decrease the amount of explicit information exchanged between them. A possible solution to this problem, is utilizing implicit information which occurs as a side-effect of robots' interactions with the environment and can be acquired via sensor measurements. This type of communication is called implicit communication.

The goal of this thesis is to completely replace explicit communication with implicit, in the object handling task, where two robots are involved. We use a decentralized leader-follower architecture. The leader's objective is to implement a desired trajectory profile, while the follower tries to keep up using only force, position and velocity measurements. Two scenarios are explored.

In the first, the cooperating agents are nonholonomic mobile robots, the object is bar and the follower-object contact is compliant. The follower uses force-torque measurements to align itself with the object and keep the contact stable. The overall system is modelled as a perturbed car-like system. Therefore, the leader, based on a robustness analysis, imposes a control scheme for the nominal car-like system.

In the second, the object is carried by mobile manipulators and all contacts are rigid. Both robots establish an impedance relation on it. The follower robustly estimates leader's desired trajectory through the motion of the object. Eventually, the position error converges to an arbitrarily small residual set containing the origin.

Keywords

Decentralized Control, Implicit Communication, Object Manipulation, Force Sensing, Leader-Follower, Nonholonomic System

Contents

Ευχαριστίες	7
Περίληψη	9
Abstract	11
List of Figures	15
1 Introduction	16
1.1 Related Work	17
2 Cooperation of mobile robots	19
2.1 System Model	20
2.1.1 Unicycle Model	20
2.1.2 Overall System	21
2.2 Follower's problem statement and control	24
2.2.1 Problem statement	24
2.2.2 Control	26
2.2.3 Simulation	30
2.3 Leader's behaviour	33
2.3.1 Chained form systems	33
2.3.2 Open loop scheme	35
2.3.3 Closed loop scheme	40
2.3.4 Closed loop scheme robustness analysis	43
2.3.5 Closed loop scheme simulation	47
3 Cooperation of mobile manipulators	52
3.1 System Model	53
3.1.1 Kinematics	54
3.1.2 Dynamics	55
3.2 Control	56
3.2.1 Feedback Linearization and Impedance Relation	56
3.2.2 Estimation law	57
3.2.3 Secondary Objectives	60
3.3 Simulation	60

4 Conclusion and future directions	62
4.1 Future directions	62
Appendices	64
A Prescribed Performance	65
B Dynamical Systems	67
Bibliography	68

List of Figures

1.1	Tight cooperation of robots	16
1.2	Types of communication	17
2.1	Cooperation of mobile robots	19
2.2	Differential wheeled robot as a unicycle	21
2.3	Overall formation with defined angles and distance	22
2.4	Compliant contact and forces exerted on the follower	22
2.5	Illustration of desired performance	26
2.6	Force error convergence	31
2.7	Torque error convergence	31
2.8	Demonstration of follower's behaviour	32
2.9	Input velocities	32
2.10	Typical convergence of leader's state.	37
2.11	Open loop forward motion	38
2.12	Angle ϕ_l in open loop forward motion	38
2.13	Open loop backward motion	39
2.14	Angle ϕ_l in open loop backward motion	39
2.15	Car's model	40
2.16	Closed loop scheme: Forward motion for positive initial θ	48
2.17	Evolution of state	48
2.18	Evolution of state in chained form	49
2.19	Evolution of linearly transformed state	49
2.20	Backward motion for positive initial θ	50
2.21	Comparison between open and closed loop	50
2.22	Forward motion for negative initial θ	51
2.23	Backward motion for negative initial θ	51
3.1	Cooperation of mobile manipulators	52
3.2	Multi-effector/object system	54
3.3	Variation	60
3.4	Original	61
3.5	Superimposed errors	61
A.1	Graphical illustration of the prescribed performance definition.	65

Chapter 1

Introduction

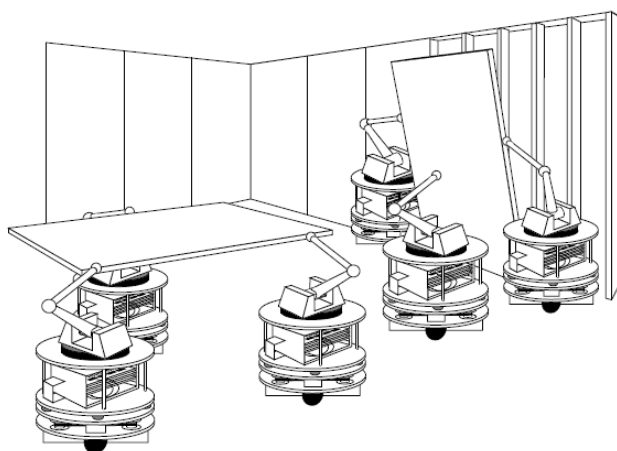


Figure 1.1: Tight cooperation of robots

The study of multirobot systems in object carrying tasks, has received increasing attention over the last decades. Using a group of robots instead of a single one, can have several advantages, such as increase in weight lifting capabilities, increase of redundancy and versatility and fault tolerance. Thus, many tasks that are impossible to execute by a single robot become feasible. Such tasks include, for instance, carrying heavy or large payloads, the assembly of multiple parts without using special fixtures, and handling of objects that are flexible or possess extra degrees of freedom.

However, new challenges arise. For example, when the number of robots becomes large, traditional approaches that rely on centralized control rapidly reach their limits and are prone to individual faults. Therefore, decentralization is necessary. Unfortunately, though, most decentralized schemes depend highly on inter-robot explicit communication (i.e. exchange of control messages or local sensory data), resulting in crowded bandwidth and requiring careful planning of communication protocols [SB00].

This thesis explores the possibility of replacing explicit communication with implicit. Explicit communication is defined as a specific act designed solely to convey

information to other robots on the team. On the other hand, implicit communication occurs as a side-effect of robots' interactions and the way they change the environment (i.e. coupling forces between the object and the robots). Implicit communication offers several immediate advantages over the explicit form. Among them are simplicity, robustness to faulty communication environments, low power consumption and stealthiness.



Figure 1.2: Types of communication

Of course, the explicit form makes teams more effective. Still, there are tasks, for which is not essential when the implicit form is available. More complex communication strategies may offer little or no benefit over low-level communication [BA94], [Don95].

We consider two types of robotic teams, the first one consisting of mobile robots and the second of mobile manipulators. The scheme is decentralized, each robot has its own controller. The architecture is of leader-follower type. Only the leader knows the desired trajectory of the object, while the follower tries to keep up using exclusively sensor information (force, position, velocity). We emphasize that the desired trajectory can neither be transmitted off-line. The only information to be exchanged, are few off-line parameters (geometric, inertial). Further information is provided in the beginning of each chapter.

1.1 Related Work

Research on cooperative manipulation began in the early 1970s. During late 1980s a strong theoretical background for the control of multi-arm robots was formed, providing the basis for research on more advanced topics from the 1990s to today (refer to [SK08]).

Some works belong in the class of centralized control. A central system obtains global information on an environment including all the robots and determines actions for all of them. In [Kha88], the overall closed-chain system is treated as an augmented object, by expressing its inertial properties via a single inertia matrix. Tanner et. al. [TLK03] proposed a centralized motion planning methodology for nonholonomic mobile manipulators, handling a deformable object, based on dipolar inverse Lyapunov functions, with guaranteed collision avoidance and convergence properties.

Another example of centralized control is the Object Impedance Control [SCJ92]. An impedance law specifies the relationship between the object's accelerations, external forces, and kinematic state. In Multiple Impedance Control [MP10] this relation is also imposed on the manipulators. Impedance control can also be based on Internal Force [BH96]. The above impedance schemes even in their decentralized versions [DCJR97] need explicit communication or off-line knowledge of the desired trajectory.

In decentralized systems, the cooperating robots do not depend on a central unit to compute their desired actions. Still, many works use explicit communication or off-line knowledge of the desired trajectory. Khatib et. al. in [KYC⁺96] extended the augmented object notion to mobile manipulators and presented a decentralized control scheme. In [LAO96], [TBK04] knowledge of the desired trajectory is required. Other decentralized schemes adopt the leader-follower architecture [LZ87],[SK98]. Since the leader has the responsibility of motion, these formations are not symmetric and thus prone to leader faults. However, to completely replace explicit communication, some agents have to be completely ignorant of the task. Therefore, this objective is only achievable with such formations.

Kosuge et. al. [KO96], [KOC97], [KOS97] designed a decentralized leader-follower scheme, in which only implicit communication is used. Only the leader knows the desired trajectory, with followers trying to estimate it through the motion of the object. The estimation scheme though, is not robust and converges only when the desired acceleration is zero. Also, object's dynamics are not explicitly dealt with.

Stilwell and Bay [SB93] studied the case of multiple nonholonomic mobile robots. The object-robot contact was modelled as a spring and damper. Again this scheme is decentralized, of leader-follower type and uses only implicit communication. The goal of the follower, is to behave as a caster (keep distance from object constant, align itself to force direction). The follower's caster behaviour is also explored in [KOS⁺98]. In the above works, it is not stated how the overall system can be stabilized.

Some decentralized schemes, which employ only implicit communication, do not include the system models and are based on decision rules over a finite set of possible actions [AHY⁺99], [YS01]. In [GMD06],[NGB⁺09] the followers take the interaction forces as input in a neural network, which produces the desired orientation and velocity as output. In [BJ95] a pushing scenario is considered, where the leader is responsible for the steering angle, while the follower only pushes. A leadership exchange scenario is explored in [PPCC02]. However, the aforementioned decision rules are mainly heuristic and there is no guarantee that the object behaves as desired.

Finally, in contrast to leader-follower architecture, in completely distributed systems all robots are equal and the task does not depend on a leader. In the pushing scenario of [RDJ95] and [DJR97] the object's motion is controlled by a quasi-static protocol. In [AN01] the task of transferring the object is divided in two tasks: constraining and moving the load. The execution of the task does not need explicit communication. However, the robots must have some knowledge about the task off-line.

Chapter 2

Cooperation of mobile robots

In this chapter the first cooperative scenario is presented. The team consists of two nonholonomic mobile robots, in a leader-follower formation and the object carried is a simple bar (fig. 2.1). Motion takes place at the horizontal plane. The nonholonomic nature of the agents increases the difficulty of the object transportation task and restricts the mobility of the overall formation. To tackle this problem we mount the object on revolute joints placed on the platforms, to allow relative angular displacements between it and the agents. The leader's joint is free, while the follower's is compliant. Moreover, the contact between the object and the follower's revolute joint is also chosen to be compliant.

As a result, the mobility is increased and force-torque exerted by the follower now depends on its relative position to the object. This enables us to introduce force-torque in the kinematic model of our system, thus removing the uncertainty in the case of purely rigid contact, where forces can only be considered at the dynamic model.

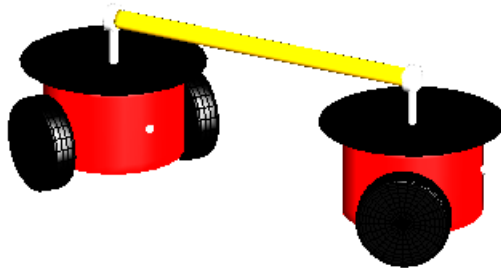


Figure 2.1: Cooperation of mobile robots

The main goal of the leader is to stabilize the position and angle of the object, while the follower is trying to keep up using only force sensing, by keeping torque

almost zero, and force almost constant, close a desired value. Follower's objectives are satisfied by employing a prescribed performance controller. As a side effect it aligns itself with the object and keeps constant inter-robot distance. With follower's goal satisfied, the overall system can be modelled as a **perturbed car-like model**, with the leader acting like the steering wheels. We discern two cases:

- Leader does not measure its free joint angle. We call this case **open loop**, since the leader has no knowledge of the overall system's state, and is rendered unable to compute steering angle. Of course, the best achievable performance is limited to leader's stabilization, with the object's angle being uncontrollable, especially in backward motion.
- Leader measures its free joint angle. We call this case **closed loop**, since the object's state is known to leader. The steering angle can now be computed. Therefore, the leader can now implement a discontinuous feedback law, which stabilizes the nominal car-like system. This law, as the robustness analysis proves, renders the system locally ultimately bounded, with region of attraction and bounds depending on follower's performance.

We emphasize, that no explicit communication is used in the above cases.

This chapter has the following structure:

- System model derivation.
- Follower's goal, control and simulation.
- Leader's control, simulation results and comparison.
 - Open loop scheme.
 - Closed loop scheme.

2.1 System Model

Both agents are differential wheeled robots. The differential wheeled robot model is equivalent to the model of the unicycle.

2.1.1 Unicycle Model

A unicycle, is a vehicle with a single orientable wheel. Its configuration is completely described by $q = [x \ y \ \theta]^T$, where (x, y) are the Cartesian coordinates of the contact point of the wheel with the ground, and θ is the orientation of the wheel with respect to the x axis. For the differential wheeled robot we can assume the same model, with the corresponding point being the middle of the wheels' axis (fig. 2.2).

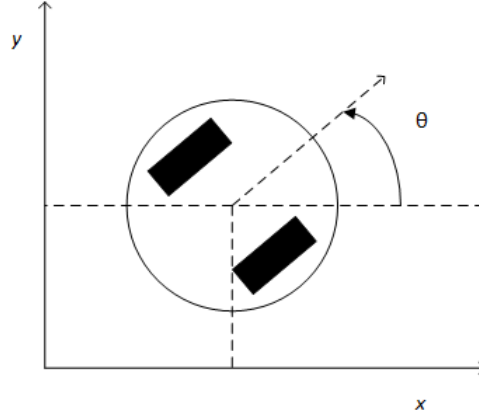


Figure 2.2: Differential wheeled robot as a unicycle

The pure rolling constraint for the wheels is expressed in the Pfaffian form as:

$$\dot{x} \sin \theta - \dot{y} \cos \theta = \begin{bmatrix} \sin \theta & -\cos \theta & 0 \end{bmatrix} \dot{q} = 0 \quad (2.1)$$

and entails that, in the absence of slipping, the velocity of the aforementioned point has zero component in the direction orthogonal to the vehicle's heading. Consider now the matrix

$$G(q) = \begin{bmatrix} g_1(q) & g_2(q) \end{bmatrix} = \begin{bmatrix} \cos \theta & 0 \\ \sin \theta & 0 \\ 0 & 1 \end{bmatrix},$$

whose columns $g_1(q)$ and $g_2(q)$ are, for each q , a basis of the null space of the matrix associated with the Pfaffian constraint. All the admissible generalized velocities at q are therefore obtained as a linear combination of $g_1(q)$ and $g_2(q)$. The kinematic model of each agent can now be described:

$$\begin{bmatrix} \dot{x}_l \\ \dot{y}_l \\ \dot{\theta}_l \end{bmatrix} = \begin{bmatrix} \cos \theta_l \\ \sin \theta_l \\ 0 \end{bmatrix} u_l + \begin{bmatrix} 0 \\ 0 \\ 1 \end{bmatrix} r_l \quad (2.2)$$

for the leader and

$$\begin{bmatrix} \dot{x}_f \\ \dot{y}_f \\ \dot{\theta}_f \end{bmatrix} = \begin{bmatrix} \cos \theta_f \\ \sin \theta_f \\ 0 \end{bmatrix} u_f + \begin{bmatrix} 0 \\ 0 \\ 1 \end{bmatrix} r_f \quad (2.3)$$

for the follower. Coordinates $x_i, y_i, \theta_i, i \in \{l, f\}$ are considered with respect to an inertial global frame.

2.1.2 Overall System

The overall formation is shown in fig. 2.3. By L we define the distance between the two robots. This distance is, indeed, not constant since it depends on the displacement of the compliant contact. We also define by θ the orientation angle of the object and by ϕ_i the angle displacement between it and the robots:

$$\phi_l = \theta_l - \theta \quad (2.4)$$

$$\phi_f = \theta - \theta_f \quad (2.5)$$

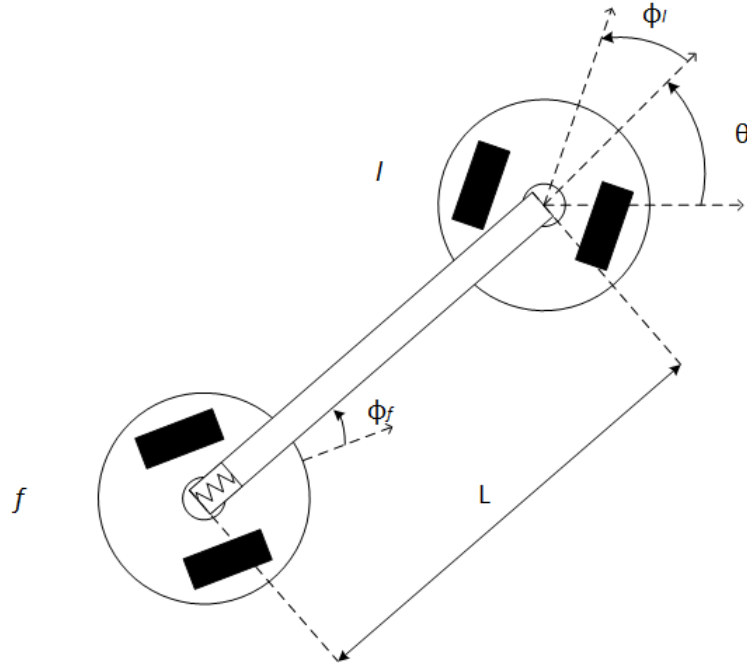


Figure 2.3: Overall formation with defined angles and distance

Contact model

The model of the contact is depicted in fig. 2.4. The forces F, T exerted on the follower are shown along with the corresponding translational δx and angular ϕ_f deformations. The translational compliance can be achieved with either a spring or a soft robot tip (see [BDR10]), with high stiffness constant. Respectively, angular compliance is implemented via a torsion spring. However, rotational stiffness constant is allowed to be more low. We stress that forces depend only on position variables, assuming that damping components are negligible.

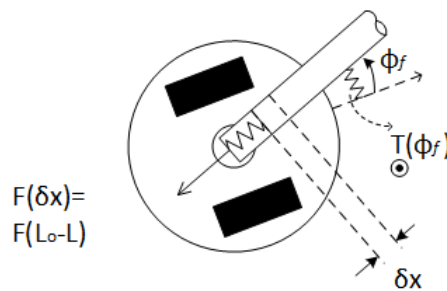


Figure 2.4: Compliant contact and forces exerted on the follower

Due to the contact's structure, the elastic force always lies on the object's direction. We assume that only compression is allowed, no stretching takes place and force magnitude is a positive strictly increasing and continuously differentiable nonlinear function of the deformation δx . Now we define the deformation

$\delta x = L_o - L$, for $L_o \geq L > \underline{L}$, where L_o is the natural inter-robot distance when deformation and consequently force are zero. \underline{L} is inter-robot distance corresponding to the highest compression possible. To summarize the above we write:

$$\mathbf{F} = \mathbf{F}(\mathbf{q}_l, \mathbf{q}_f, \theta) = F(L_o - L) \begin{bmatrix} \cos \theta \\ \sin \theta \end{bmatrix} \quad (2.6)$$

$$0 \leq F(L_o - L) < \bar{F} = F(L_o - \underline{L}) \quad (2.7)$$

$$\frac{\partial F}{\partial \delta x} > 0 \text{ and } \frac{\partial F}{\partial L} = -\frac{\partial F}{\partial \delta x} < 0 \quad (2.8)$$

$$F(0) = 0 \quad (2.9)$$

Other than the previous properties, no exact knowledge about the force model is available.

Torque, indeed, is orthogonal to the horizontal plane and its magnitude is also a positive strictly increasing and continuously differentiable nonlinear function of the angle ϕ_f . We also write:

$$T = T(\phi_f) \quad (2.10)$$

$$\frac{\partial T}{\partial \phi_f} > 0 \quad (2.11)$$

$$T(0) = 0 \quad (2.12)$$

ϕ_f is not restricted naturally. However, as described below, follower constraints it inside the interval $(-\frac{\pi}{2}, \frac{\pi}{2})$, in order to avoid singular configurations. Therefore, whereas the exact torque function is unknown we need to estimate values $T(\pm\frac{\pi}{2})$.

Model derivation

We use unicycle equations (2.2,2.3) along with the following:

$$L = \sqrt{(x_l - x_f)^2 + (y_l - y_f)^2} \quad (2.13)$$

$$\begin{bmatrix} x_f \\ y_f \end{bmatrix} = \begin{bmatrix} x_l \\ y_l \end{bmatrix} - L \begin{bmatrix} \cos \theta \\ \sin \theta \end{bmatrix} \quad (2.14)$$

Differentiating the above and after some manipulations we arrive at:

$$\dot{\theta} = \frac{u_l \sin \phi_l}{L} + \frac{u_f \sin \phi_f}{L} \quad (2.15)$$

$$\dot{L} = -u_f \cos \phi_f + u_l \cos \phi_l \quad (2.16)$$

$$\dot{\phi}_f = -r_f + \frac{u_l \sin \phi_l}{L} + \frac{u_f \sin \phi_f}{L} \quad (2.17)$$

Follower's control scheme is based on force-torque sensing and control. Hence, it is reasonable to express the state equations with respect to the compliant contact's forces. Differentiating force and torque magnitude: $\dot{F} = \frac{\partial F}{\partial L} \dot{L}$ and $\dot{T} = \frac{\partial T}{\partial \phi_f} \dot{\phi}_f$ we

can finally complete state equations. The overall system model is described below:

$$\begin{bmatrix} \dot{x}_l \\ \dot{y}_l \\ \dot{\theta}_l \\ \dot{\theta} \\ \dot{F} \\ \dot{T} \end{bmatrix} = \begin{bmatrix} u_l \cos \theta_l \\ u_l \sin \theta_l \\ r_l \\ \frac{u_l \sin \phi_l}{L} + \frac{u_f \sin \phi_f}{L} \\ \frac{\partial F}{\partial L} (-u_f \cos \phi_f + u_l \cos \phi_l) \\ \frac{\partial T}{\partial \phi_f} \left(-r_f + \frac{u_l \sin \phi_l}{L} + \frac{u_f \sin \phi_f}{L} \right) \end{bmatrix} \quad (2.18)$$

We could replace θ_l with ϕ_l in some cases, for example in the closed loop scheme.

2.2 Follower's problem statement and control

2.2.1 Problem statement

Force

Follower's goal is to keep force almost constant close to a desired value. Satisfaction of this goal establishes enough force for the stability of the contact. It also guarantees safety by limiting too high forces. We could describe the goal:

$$0 < F - F_d < \rho_f(t) < \bar{F} - F_d$$

where F_d is the desired force. Function $\rho_f(t)$ is called a performance function (for more information refer to Appendix A or [BR10]). It acts as an upper bound for the force error $F - F_d$. We can achieve desired transient and steady-state properties of the error, by choosing an appropriate performance function. A common choice is an exponentially decaying function $\rho(t) = (\rho_o - \rho_\infty)e^{-kt} + \rho_\infty$. Note that this upper bound must be less than the maximum force error. Moreover, to ensure contact is not lost, this error is only allowed to be positive. If we define $e_f = F - F_d - \frac{\rho_f}{2}$ the goal can also be written in the form:

$$|e_f| < \frac{\rho_f}{2} \quad (2.19)$$

Remark 2.1. *Satisfaction of force goal has the side-effect of keeping steady-state distance between leader and follower, almost constant. Thus, follower manages to keep up with the leader and maintains contact.*

Since function $F(L_o - L)$ is continuous, strictly increasing w.r.t. $L_o - L$, and $F(0) = 0$:

$$L_o - L_d < L_o - L < F^{-1}(F_d + \rho_f)$$

Thus if ρ_∞ is sufficiently small, using Taylor expansion:

$$\begin{aligned} 0 < L_o - L < L_o - L_d - \frac{\partial F^{-1}}{\partial L} \rho_f + o(\rho_f) \\ 0 < \lim_{t \rightarrow \infty} (L_d - L) < \left| \frac{\partial F}{\partial L} \right|^{-1} \rho_{f\infty} + o(\rho_{f\infty}) \end{aligned} \quad (2.20)$$

Considering $\left|\frac{\partial F}{\partial L}\right| \neq 0$ steady-state error can be made arbitrarily small by choosing steady-state performance value $\rho_{f\infty}$.

Remark 2.2. *If stiffness constant $\left|\frac{\partial F}{\partial L}\right|$ is very high, not only steady-state, but also transient-state distance is almost constant.*

Using Taylor expansion:

$$F(L_o - L) \approx -\frac{\partial F}{\partial L}(L_o - L)$$

Hence, replacing the above into (2.19) we obtain:

$$0 < L_o - L < \frac{\rho_f}{\left|\frac{\partial F}{\partial L}\right|} + \frac{F_d}{\left|\frac{\partial F}{\partial L}\right|} \quad (2.21)$$

Torque

Regarding torque, follower has the goal to keep it close to zero. Additionally torque is not allowed to reach value $T\left(\pm\frac{\pi}{2}\right)$, in order to avoid singular configurations. Again, a performance function is used, with the following properties:

$$|T| = |e_\tau| < \rho_\tau(t) \leq \bar{T} < \left|T\left(\pm\frac{\pi}{2}\right)\right| \quad (2.22)$$

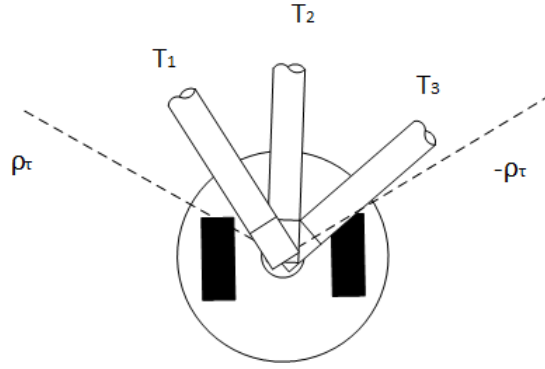
where, \bar{T} is the maximum allowed torque and can be chosen to be any value within the interval $(|T(\phi_f(0))|, |T(\pm\frac{\pi}{2})|)$, assuming that initial configuration is not singular: $|\phi_f(0)| < \frac{\pi}{2}$. This is the reason, knowledge of $T\left(\pm\frac{\pi}{2}\right)$ is required.

Remark 2.3. *The side-effect of torque goal satisfaction is the alignment of the follower to the object, with arbitrarily small steady-state error.*

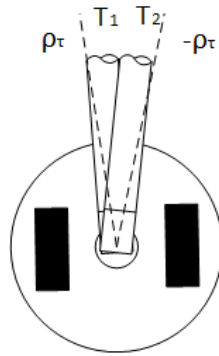
Indeed, since function T is continuous, strictly increasing, and $T(0) = 0$:

$$\begin{aligned} |\phi_f(t)| &< T^{-1}(\rho_\tau(t)) \text{ and as a result} \\ \lim_{t \rightarrow \infty} |\phi_f(t)| &< T^{-1}(\rho_{\tau\infty}) \end{aligned} \quad (2.23)$$

which again can be made arbitrarily small. The above can be illustrated in the following figures:



(a) Transient state



(b) Close to steady-state

Figure 2.5: All possible configurations have lower torque than the performance function: $|T_i| < \rho_\tau$. As a side effect, angle is also bounded inside a continuously shrinking sector. Implicitly, follower aligns itself to the object.

Remark 2.4. *Another side-effect of follower's actions is that the system model approximates that of a car-like robot with front wheel actuation.*

At steady state L is almost constant and ϕ_f is very small, so object's angular equation (2.15) can be approximated by:

$$\dot{\theta} \approx \frac{u_l \sin \phi_l}{L} \quad (2.24)$$

2.2.2 Control

Before we proceed with the controller presentation, some assumptions must be made:

Assumption 2.1. *The initial force and torque error satisfy $|e_f(0)| < \frac{\rho_f(0)}{2}$ and $|e_\tau(0)| < \rho_\tau(0)$.*

This can easily be achieved by choosing values ρ_{fo} , $\rho_{\tau o}$.

Assumption 2.2. *The initial configuration is in the region $|\phi_f(0)| < \frac{\pi}{2}$, hence torque error satisfies $|T(\phi_f(0))| < |T(\pm \frac{\pi}{2})|$.*

This enables us to choose maximum allowed torque \bar{T} in (2.22) when we define performance bounds. If this assumption is violated it is trivial for the follower to reconfigure its position, before the overall system begins execution of its task.

Assumption 2.3. *Initial force is higher than the desired force: $F(L(0)) > F_d$.*

Again, it is trivial for the follower to reconfigure its position before execution, if initial force is lower.

Control Scheme

After choosing suitable performance functions we can finally design the desired velocities:

$$u_f = -k_f \ln \left(\frac{1 + \frac{2e_f}{\rho_f(t)}}{1 - \frac{2e_f}{\rho_f(t)}} \right) \quad (2.25)$$

$$r_f = k_\tau \ln \left(\frac{1 + \frac{e_\tau}{\rho_\tau(t)}}{1 - \frac{e_\tau}{\rho_\tau(t)}} \right) \quad (2.26)$$

Remark 2.5. *In contrast to most decentralized schemes, the proposed is independent of leader's velocity inputs u_l, r_l . Therefore, no explicit communication is takes place. The sacrifice for this lack of knowledge is that ultimate boundedness of force-torque errors is achieved instead of asymptotic stability. However, error can converge to an arbitrarily small residual set, through choice of $\rho_{i\infty}$*

Stability Analysis

Theorem 2.1. *Consider the force-torque equations of the follower (2.18) with initial values satisfying Assumptions 2.1-2.3. Provided leader's input velocity u_l is smooth, bounded, with bounded derivatives, control scheme (2.25), (2.26) maintains satisfaction of constraints (2.19), (2.22).*

Proof: First, let us define the normalized errors:

$$\xi_f = \frac{2e_f}{\rho_f(t)} \quad (2.27)$$

$$\xi_\tau = \frac{e_\tau}{\rho_\tau(t)} \quad (2.28)$$

In this respect, desired velocities (2.25)-(2.26) may be written as functions of the normalized errors $\xi_i, i \in \{f, \tau\}$ as follows:

$$u_f = -k_f \ln \left(\frac{1 + \xi_f}{1 - \xi_f} \right) \quad (2.29)$$

$$r_f = k_\tau \ln \left(\frac{1 + \xi_\tau}{1 - \xi_\tau} \right) \quad (2.30)$$

Next, we define the overall ξ vector:

$$\xi = [\xi_f \quad \xi_\tau]^T \quad (2.31)$$

Differentiating the normalized errors with respect to time and substituting (2.18), we obtain in a compact form, the dynamical system of the overall state vector:

$$\dot{\xi} = h(t, \xi) \quad (2.32)$$

where the function $h(t, \xi)$ includes all terms found at the right hand side after the differentiation of ξ . Let us also define the open set:

$$\Omega_\xi = (-1, 1) \times (-1, 1)$$

The proof proceeds in two phases. First, the existence of a maximal solution $\xi(t)$ of (2.32) over the set Ω_ξ for a time interval $[0, \tau_{\max})$ (i.e., $\xi(t) \in \Omega_\xi, \forall t \in [0, \tau_{\max})$) is ensured. Then, we prove that the proposed control scheme guarantees, for all $t \in [0, \tau_{\max})$: a) the boundedness of all closed loop signals of (2.32) as well as that b) $\xi(t) \in \Omega'_\xi$ with Ω'_ξ denoting a compact subset of Ω_ξ , which subsequently leads by contradiction with Proposition B.1 (Appendix B) to $\tau_{\max} = \infty$. Hence, from (2.27)-(2.28), we conclude that:

$$\begin{aligned} -\frac{\rho_f(t)}{2} < e_f(t) < \frac{\rho_f(t)}{2} \\ -\rho_\tau(t) < e_\tau(t) < \rho_\tau(t) \end{aligned}$$

for all $t \geq 0$ and consequently that satisfaction of force-torque constraints with prescribed performance is achieved.

Phase A: Set Ω_ξ is nonempty and open. Moreover, owing to the selection of the performance functions $\rho_i(t)$, as well as to assumptions we conclude that $\xi(0) \in \Omega_\xi$. Additionally, due to the smoothness of a) the system nonlinearities, b) leader's velocity and c) the proposed control scheme, over Ω_ξ , it can be easily verified that $h(t, \xi)$ is continuous on t and continuous for all $\xi \in \Omega_\xi$. Therefore, the hypotheses of Theorem B.1 stated in Appendix B hold and the existence of a maximal solution $\xi(t)$ of (2.32) on a time interval $[0, \tau_{\max})$ such that $\xi(t) \in \Omega_\xi, \forall t \in [0, \tau_{\max})$ is ensured.

Phase B: We have proven in Phase A that $\xi(t) \in \Omega_\xi, \forall t \in [0, \tau_{\max})$ or equivalently that:

$$\xi_i(t) \in (-1, 1), i \in \{f, \tau\} \quad (2.33)$$

for all $t \in [0, \tau_{\max})$. Therefore, the signals:

$$\varepsilon_i(t) = \ln \left(\frac{1 + \xi_i(t)}{1 - \xi_i(t)} \right), i \in \{f, \tau\} \quad (2.34)$$

are well defined for all $t \in [0, \tau_{\max})$.

Consider now the positive definite and radially unbounded function $V_f = \frac{1}{2}\varepsilon_f^2$. Differentiating with respect to time, we obtain:

$$\begin{aligned} \dot{V}_f &= \frac{\partial F}{\partial L} \frac{4\varepsilon_f}{(1 - \xi_f^2) \rho_f(t)} (-u_f \cos \phi_f + u_l \cos \phi_l \\ &\quad - \left(\frac{\partial F}{\partial L} \right)^{-1} (1 + \xi_f) \frac{\dot{\rho}_f(t)}{2}). \end{aligned} \quad (2.35)$$

Substituting u_f from (2.25) then:

$$\begin{aligned} \dot{V}_f &= \frac{\partial F}{\partial L} \frac{4\varepsilon_f}{(1 - \xi_f^2) \rho_f(t)} (k_f \varepsilon_f \cos \phi_f + u_l \cos \phi_l \\ &\quad - \left(\frac{\partial F}{\partial L} \right)^{-1} (1 + \xi_f) \frac{\dot{\rho}_f(t)}{2}). \end{aligned} \quad (2.36)$$

Since $\dot{u}_l, \dot{\rho}_f$ are bounded by construction, $\xi \in \Omega_c$ and stiffness constant $\frac{\partial F}{\partial L} \leq c < 0$ is nonzero we arrive at:

$$\left| u_l \cos \phi_l - \left(\frac{\partial F}{\partial L} \right)^{-1} (1 + \xi_f) \frac{\dot{\rho}_f(t)}{2} \right| \leq \bar{U}_f \quad (2.37)$$

where

$$\bar{U}_f = |u_l| + \frac{1}{c} |\dot{\rho}_f| \quad (2.38)$$

Moreover, $\cos(\phi_f) > \cos(\bar{\phi}) > 0$, $\rho_f > 0$ and $\xi_f < 1$, where $\bar{\phi} = T^{-1}(\bar{T}) < \frac{\pi}{2}$ is the maximum allowed value for ϕ_f . Therefore $\dot{V}_f < 0$ when $|\varepsilon_f(t)| > \frac{\bar{U}_f}{k_f \cos(\bar{\phi})}$ and subsequently:

$$|\varepsilon_f(t)| \leq \bar{\varepsilon}_f = \max \left\{ |\varepsilon_f(0)|, \frac{\bar{U}_f}{k_f \cos(\bar{\phi})} \right\}, \quad (2.39)$$

for all $t \in [0, \tau_{\max})$. Taking the inverse of (2.34):

$$-1 < \frac{e^{-\bar{\varepsilon}_f} - 1}{e^{-\bar{\varepsilon}_f} + 1} = \underline{\xi}_f \leq \xi_f(t) \leq \bar{\xi}_f = \frac{e^{\bar{\varepsilon}_f} - 1}{e^{\bar{\varepsilon}_f} + 1} < 1 \quad (2.40)$$

for all $t \in [0, \tau_{\max})$. As a result, velocity u_f remains bounded (i.e., $|u_f(t)| \leq k_f \bar{\varepsilon}_f$) for all $t \in [0, \tau_{\max})$. Following similar analysis, using $V_\tau = \frac{1}{2}\varepsilon_\tau^2$ we obtain:

$$|\varepsilon_\tau(t)| \leq \bar{\varepsilon}_\tau = \max \left\{ |\varepsilon_\tau(0)|, \frac{\bar{U}_\tau}{k_\tau \cos(\bar{\psi})} \right\} \quad (2.41)$$

for $t \in [0, t_{\max})$ and an unknown positive constant \bar{U}_τ . As before, taking the inverse logarithmic function:

$$-1 < \frac{e^{-\bar{\varepsilon}_\tau} - 1}{e^{-\bar{\varepsilon}_\tau} + 1} = \underline{\xi}_\tau \leq \xi_\tau(t) \leq \bar{\xi}_\tau = \frac{e^{\bar{\varepsilon}_\tau} - 1}{e^{\bar{\varepsilon}_\tau} + 1} < 1 \quad (2.42)$$

and velocity r_f remains bounded (i.e., $|r_f(t)| \leq k_\tau \bar{\varepsilon}_\tau$) for all $t \in [0, \tau_{\max})$.

Up to this point, what remains to be shown is that $\tau_{\max} = \infty$. Notice that (2.40) and (2.42) imply that $\xi(t) \in \Omega'_\xi, \forall t \in [0, \tau_{\max})$, where:

$$\Omega'_\xi = \prod_{i \in \{f, \tau\}} \left[\frac{e^{-\bar{\varepsilon}_i} - 1}{e^{-\bar{\varepsilon}_i} + 1}, \frac{e^{\bar{\varepsilon}_i} - 1}{e^{\bar{\varepsilon}_i} + 1} \right]$$

is a nonempty and compact set. Moreover, it can be easily verified that:

$$\Omega'_\xi \subset \Omega_\xi$$

Hence, assuming $\tau_{\max} < \infty$ and since $\Omega'_\xi \subset \Omega_\xi$, Proposition B.1 in Appendix B dictates the existence of a time instant $t' \in [0, \tau_{\max})$ such that $\xi(t') \notin \Omega'_\xi$, which is a clear contradiction. Therefore, $\tau_{\max} = \infty$. As a result, all closed loop signals remain bounded and moreover $\xi(t) \in \Omega'_\xi \subset \Omega_\xi, \forall t \geq 0$. Finally, from (2.27), (2.28), (2.40) and (2.42), we conclude that:

$$\begin{aligned} 0 < (\underline{\xi}_f + 1) \frac{\rho_f(t)}{2} \leq F(t) - F_d \leq (\bar{\xi}_f + 1) \frac{\rho_f(t)}{2} < \rho_f(t) \\ -\rho_\tau(t) < \underline{\xi}_\tau \rho_\tau(t) \leq e_\tau(t) \leq \bar{\xi}_\tau \rho_\tau(t) < \rho_\tau(t) \end{aligned}$$

for all $t \geq 0$ and consequently follower's goal is achieved, as presented in subsection 2.2.1, which completes the proof.

Remark 2.6. *From the aforementioned proof, it is worth noticing that the proposed control scheme achieves its goals without resorting to the need of rendering $\bar{\varepsilon}_i, i \in \{f, \tau\}$ arbitrarily small, through extreme values of the control gains k_i . In this spirit, large leader velocity affects only the size of $\bar{\varepsilon}_i$, but leaves unaltered the achieved stability properties as shown in the above equations. Moreover, the selection of the control gains k_i is significantly simplified to adopting those values that lead to reasonable control effort.*

2.2.3 Simulation

This simulation is carried out to illustrate only follower's behaviour. Overall system behaviour does not concern us in this section. We only intend to demonstrate how performance bounds are met.

A simple scenario is considered (fig. 2.8), in which leader makes two steering manoeuvres of 90° . We design the follower's controller according to (2.25)-(2.26). The system starts from the initial configuration: $x_l(0) = 2, y_l(0) = 0, \phi_l(0) = 0, \theta(0) = \frac{\pi}{8}, F(0) = 40, T(0) = 8$. To model the force and torque we used models: $F = 500(L - L_0), T = 40 \sin \phi_f$. The desired force is $F_d = 10$. With maximum allowed force $\bar{F} = 50$, maximum allowed torque $\bar{T} = 30$, steady state errors 0.1 and minimum convergence rate $e^{-0.5t}$, we choose the performance functions: $\rho_f = (50 - 0.1)e^{-0.5t} + 0.1, \rho_\tau = (30 - 0.1)e^{-0.5t} + 0.1$. Finally, we choose $k_f = 0.1, k_\tau = 0.1$.

As depicted in figures 2.6, 2.7, satisfaction of force and torque constraints is achieved. Also convergence rate of force/torque errors to their steady state residual

sets is high enough. Disturbances caused by the unpredictable leader's movement are rejected effectively. Implicitly follower succeeds in keeping up with the leader (fig.2.8). Additionally, control effort is satisfactorily smooth and comparable to leader's effort (fig. 2.9).

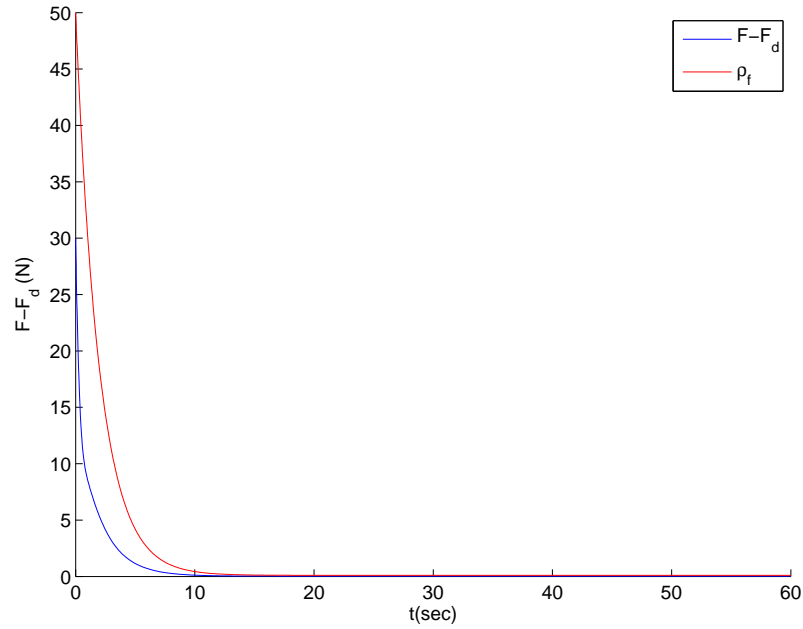


Figure 2.6: Force error convergence

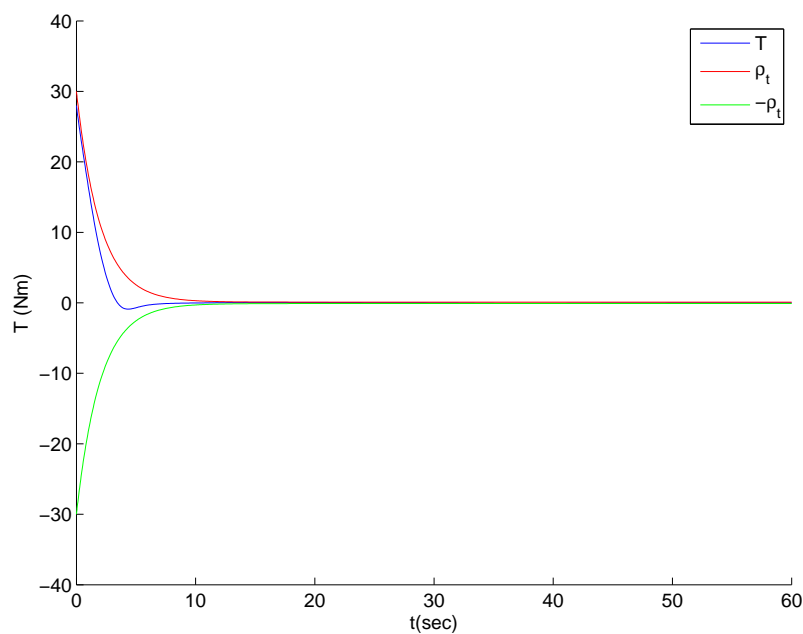


Figure 2.7: Torque error convergence

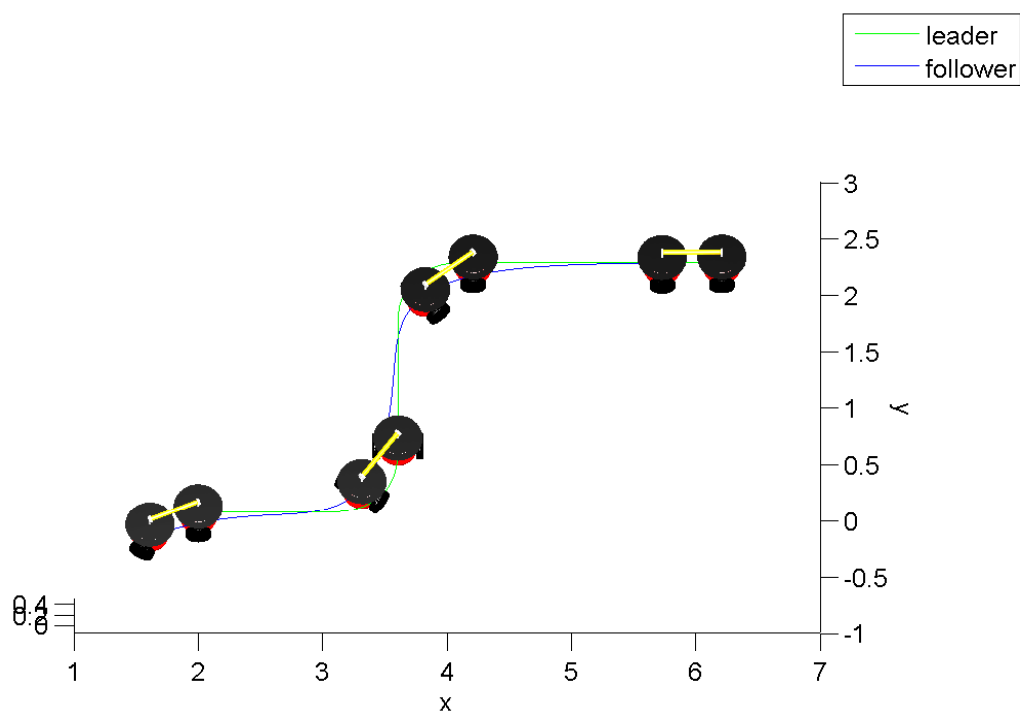


Figure 2.8: Demonstration of follower's behaviour. Coloured contours are the robots' trajectories. Satisfaction of force-torque goals results in contact maintenance and follower's alignment to the object.

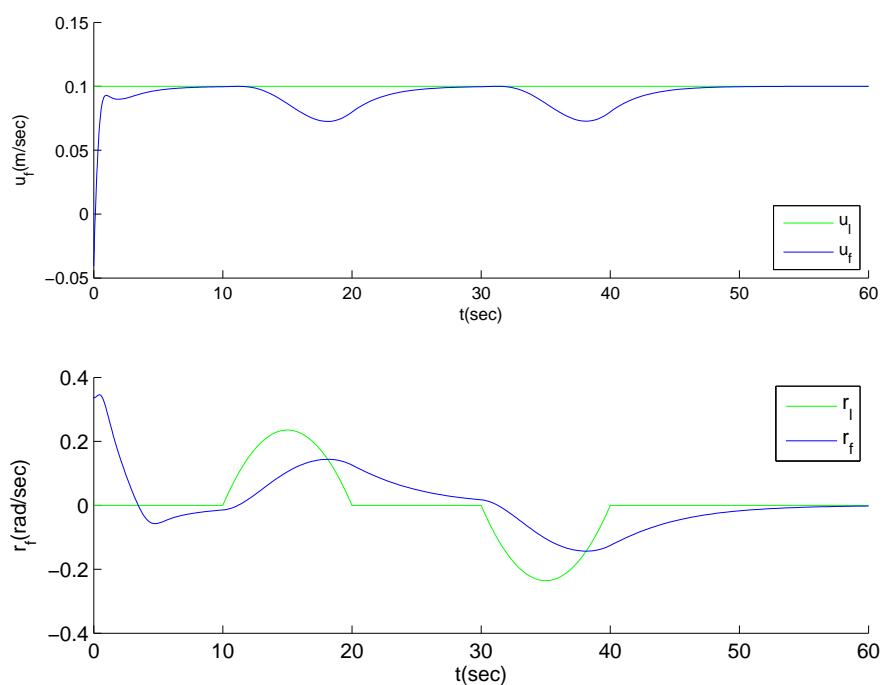


Figure 2.9: Input velocities. Follower does not overreact to leader's movement.

2.3 Leader's behaviour

In the previous section, we examined the overall system from the perspective of the follower. Now it follows naturally to highlight leader's possible actions. In the beginning of this chapter, it was stated that we discern two cases, depending on availability of ϕ_l sensing. The first case, in which this signal cannot be measured, is called open loop. Leader has information about its own position variables x_l, y_l, θ_l . On the other hand, in the second-closed loop case, leader has also knowledge of ϕ_l . We intend to show that the latter scheme outperforms the former one.

In both cases, we consider the position stabilization problem. We desire to drive the system from an initial to a goal configuration (i.e. the origin). For the open loop scheme, only the unicycle model of the leader is considered, whereas for the closed loop a perturbed car-like model of the overall system is derived. Such non-holonomic systems, can only be stabilized via either time-varying or discontinuous state feedback control. In this work we follow the second approach. The synthesis of a simple discontinuous law is derived, when the system is in the so-called chained form (see [Ast95]). Before we proceed, we present some preliminaries about chained form systems.

2.3.1 Chained form systems

This class of nonholonomic systems is described by equations of the form:

$$\begin{aligned}
 \dot{z}_1 &= v_1 \\
 \dot{z}_2 &= v_2 \\
 \dot{z}_3 &= z_2 v_1 \\
 \dot{z}_4 &= z_3 v_1 \\
 &\dots \\
 \dot{z}_n &= z_{n-1} v_1
 \end{aligned} \tag{2.43}$$

Such systems are maximally nonholonomic, i. e. are completely controllable, thus it is possible to find a pair of control signal v_1 and v_2 steering the state of the system (2.43) to any configuration. However, for general nonlinear systems controllability does not imply smooth stabilizability [Bro83] and in fact this system cannot be stabilized through continuously differentiable, state feedback control. It is possible, though, to stabilize system (2.43) via a discontinuous state feedback control law. This law is derived from the following lemma [Ast95].

Lemma 2.1. *The system of ordinary differential equations:*

$$\begin{aligned}
 \dot{z}_1 &= -kz_1 \\
 \dot{z}_2 &= p_2 z_2 + p_3 \frac{z_3}{z_1} + \dots + p_{n-1} \frac{z_{n-1}}{z_1^{n-3}} + p_n \frac{z_n}{z_1^{n-2}} \\
 \dot{z}_3 &= -kz_1 z_2 \\
 &\dots \\
 \dot{z}_{n-1} &= -kz_1 z_{n-2} \\
 \dot{z}_n &= -kz_1 z_{n-1}
 \end{aligned} \tag{2.44}$$

with initial condition:

$$z(0) = [z_1(0) \quad z_2(0) \quad z_3(0) \quad \dots \quad z_n(0)]$$

such that:

$$z_1(0) \neq 0 \quad (2.45)$$

has a unique and well defined solution for all $t \geq 0$.

Moreover, let

$$\Lambda = \begin{bmatrix} p_2 & p_3 & p_4 & \dots & p_{n-1} & p_n \\ -k & k & 0 & \dots & 0 & 0 \\ 0 & -k & 2k & \dots & 0 & 0 \\ \vdots & \vdots & \vdots & \vdots & \vdots & \vdots \\ 0 & 0 & 0 & \dots & (n-3)k & 0 \\ 0 & 0 & 0 & \dots & -k & (n-2)k \end{bmatrix} \quad (2.46)$$

and

$$\Phi(t) = \exp(\Lambda t)$$

Then the unique solution of the system satisfying the initial condition constraint (2.45) is:

$$\begin{aligned} z_1(t) &= z_1(0) e^{-kt} \\ \begin{bmatrix} z_2(t) \\ z_3(t) \\ \vdots \\ z_{n-1}(t) \\ z_n(t) \end{bmatrix} &= \Gamma(t) \Phi(t) \xi(0) \end{aligned} \quad (2.47)$$

where

$$\xi(0) = \left[z_2(0) \quad \frac{z_3(0)}{z_1(0)} \quad \dots \quad \frac{z_{n-1}(0)}{z_1^{n-3}(0)} \quad \frac{z_n(0)}{z_1^{n-2}(0)} \right]^T \quad (2.48)$$

and

$$\Gamma(t) = \text{diag}(1, z_1(t), \dots, z_1^{n-3}(t), z_1^{n-2}(t))$$

Proof. For the component z_1 the proof is trivial. Regarding the remaining components of the state vector, note that if $z_1 \neq 0$ it is possible to apply the state transformation:

$$\xi = \begin{bmatrix} \xi_2(t) \\ \xi_3(t) \\ \vdots \\ \xi_{n-1}(t) \\ \xi_n(t) \end{bmatrix} = \begin{bmatrix} \frac{z_2(t)}{z_1(t)} \\ \frac{z_3(t)}{z_1(t)} \\ \vdots \\ \frac{z_{n-1}(t)}{z_1^{n-3}(t)} \\ \frac{z_n(t)}{z_1^{n-2}(t)} \end{bmatrix} \quad (2.49)$$

yielding

$$\dot{\xi} = \Lambda \xi \quad (2.50)$$

System (2.50), with the initial conditions (2.48), admits the closed integral

$$\xi(t) = \Phi(t) \xi(0).$$

Hence, the claim directly follows, applying the inverse transformation. \square

The result of this lemma allows us to prove the following.

Proposition 2.1. *Consider the system (2.43) and assume that its initial state z_0 satisfies condition (2.45). Then the discontinuous control law equation:*

$$v = \begin{bmatrix} -kz_1 \\ p_2 z_2 + p_3 \frac{z_3}{z_1} + \cdots + p_{n-1} \frac{z_{n-1}}{z_1^{n-3}} + p_n \frac{z_n}{z_1^{n-2}} \end{bmatrix} \quad (2.51)$$

exponentially drives the state to the origin of the coordinates system if

$$k > 0 \quad \sigma(\Lambda) \subset C^- \quad (2.52)$$

where Λ is defined in (2.46), $\sigma(\Lambda)$ denotes the spectrum of the matrix Λ and C^- denotes the open left-half complex plane.

Proof. It follows directly from lemma 2.1. In fact if $k > 0$ the state z_1 converges exponentially to zero and as a consequence the matrix $\Gamma(t)$ is well defined and bounded for all $t \geq 0$. Moreover, the vector $\xi(0)$ is bounded and if Λ is a Hurwitz matrix, states z_2 through z_n , tend to zero with an exponential decay rate. \square

Remark 2.7. *The assumption $z_1(0) \neq 0$ can be done without lack of generality, as it is always possible to apply preventively an open loop control input, driving the system arbitrarily away from the plane $z_1 = 0$.*

Remark 2.8. *Simple algebra shows that, if $k \neq 0$, it is always possible to fix the coefficients p_i such that the matrix Λ is Hurwitz.*

Remark 2.9. *It must be noticed that the discontinuous control law (2.51) does not provide an exponential stabilizer in the usual sense. As a matter of fact, it guarantees only exponential convergence of the state to the origin. Such a convergence takes place only for initial conditions in an open and dense set, namely in all \mathbb{R}^n without the plane $z_1 = 0$. For this reason we can refer to the control law (2.51) as a global almost exponential stabilizer.*

Remark 2.10. *Note that, under the hypotheses of Proposition 2.1 and if $z_1(0) \neq 0$, the control signal (2.51) is bounded, along the trajectories of the closed loop system, for all $t \geq 0$ and decays exponentially to zero.*

2.3.2 Open loop scheme

As stated before, the desired task is point stabilization of the leader's state. Without loss of generality, this point is the origin of the coordinate system. To achieve this goal we consider the chained form model of the unicycle, and use the

aforementioned discontinuous control law (2.51). A way (not unique) to transform the unicycle model to chained form is presented below.

$$\begin{aligned} z_1 &= x_l \\ z_2 &= \tan \theta_l \\ z_3 &= y_l \end{aligned} \tag{2.53}$$

with inputs:

$$\begin{aligned} u_l &= \frac{v_1}{\cos \theta_l} \\ r_l &= v_2 \cos^2 \theta_l \end{aligned} \tag{2.54}$$

Applying Proposition 2.1, we obtain

$$\begin{aligned} u_l &= -k \frac{x_l}{\cos \theta_l} \\ r_l &= \cos^2 \theta_l \left(p_2 \tan \theta_l + p_3 \frac{y_l}{x_l} \right) \end{aligned} \tag{2.55}$$

Stability of object's angle

Remark 2.11. *During forward motion, angle ϕ_l is bounded for turning radius and forward velocity large enough: $u_l > cL|r_l| + \epsilon$, where c, ϵ are positive constants with $c > 1$ and ϵ large enough. During backward motion, though, this degree of freedom is unstable in the absence of feedback and renders the system prone to singular configurations.*

Indeed, from equations (2.2),(2.15) we obtain:

$$\dot{\phi}_l = r_l - \frac{u_l \sin \phi_l}{L} - \frac{u_f \sin \phi_f}{L} \tag{2.56}$$

Recall that since follower satisfies force-torque constraints the last term at steady state $\left| \frac{u_f \sin \phi_f}{L} \right| < \delta$, where δ is an arbitrarily small constant (eq. 2.39, 2.38, 2.23). Suppose now, that the aforementioned condition holds with $\epsilon > \delta L$. Next, take Lyapunov function $V = \frac{1}{2} \phi_l^2$. Differentiating it we arrive at:

$$\dot{V} \leq \phi_l \left(r_l + \delta - \left(c|r_l| + \frac{\epsilon}{L} \right) \sin \phi_l \right)$$

As a result:

$$\begin{aligned} \dot{V} &< 0, \text{ for } |\phi_l| > \bar{\phi}_l \\ \bar{\phi}_l &= \max \sin^{-1} \left(\frac{r_l + \delta}{c|r_l| + \frac{\epsilon}{L}} \right) \end{aligned} \tag{2.57}$$

This property is due to the open loop architecture and is independent of the control scheme. One possible way to achieve the remark's condition with this specific control law (2.55) is to choose proper gains k, p_i , such that states z_2, z_3 converge to zero

faster than state z_1 . Furthermore, (2.55) must be slightly modified, to prevent u_l from reaching ϵ :

$$\begin{bmatrix} u_l & r_l \end{bmatrix} = \begin{cases} \text{control law (2.55) if } |kx_l| > \epsilon \\ \begin{bmatrix} 0 & 0 \end{bmatrix}^T \text{ if } |kx_l| \leq \epsilon \end{cases}$$

On the contrary, during backward motion $u_l < 0$ and thus, product $(-u_l \phi_l \sin \phi_l)$ is positive, rendering stabilization of angle ϕ_f very difficult without feedback. For example if $r_l = 0$, $\dot{V} \geq 0$ for $\phi_l > \epsilon$, where ϵ is a very small constant.

From the above, it is clear that angle ϕ_l not only is not stabilizable, but can be unbounded as well. These problems are illustrated in the following simulations.

Simulation

We simulate the performance of the overall system, while the leader executes its stabilization control law. We test both movement directions (forward, backward). For the follower we use the same parameters as in subsection 2.2.3, except for gains, which are chosen $k_f = k_\tau = 1$. Leader's goal configuration is the origin, with zero heading angle.

In figure 2.10 it is shown how leader's state variables exponentially converge to zero with this control law. Forward motion behaviour is depicted in figures 2.11, 2.12. Notice that angle ϕ_l remains bounded since no sharp turn take place. Finally, in figures 2.13, 2.14 backward motion behaviour is shown. Angle ϕ_l is unbounded and escapes region $(-\frac{\pi}{2}, \frac{\pi}{2})$.

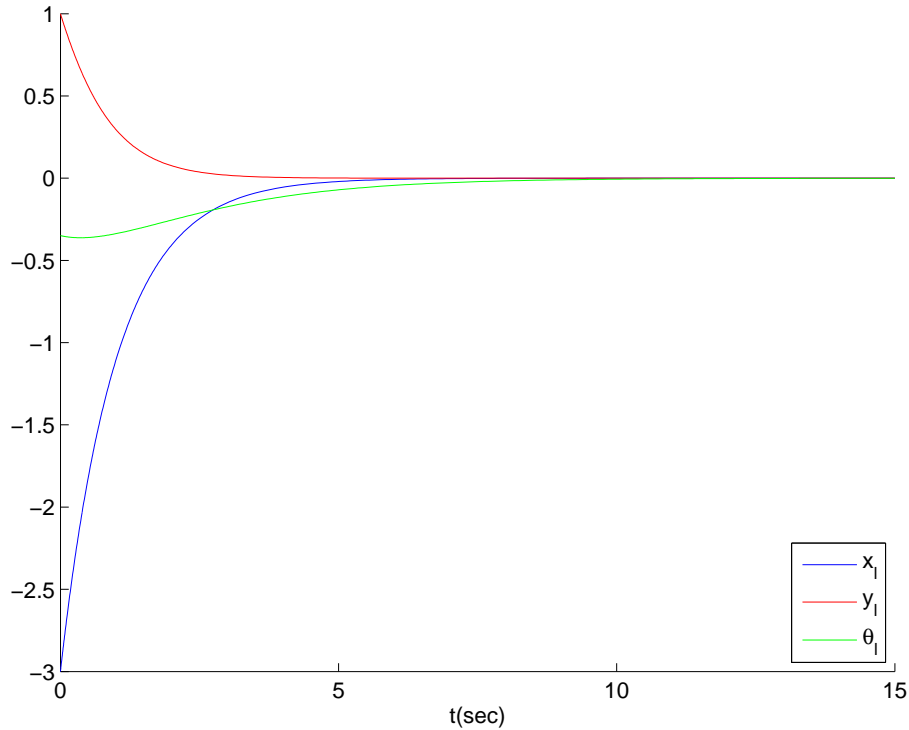


Figure 2.10: Typical convergence of leader's state.

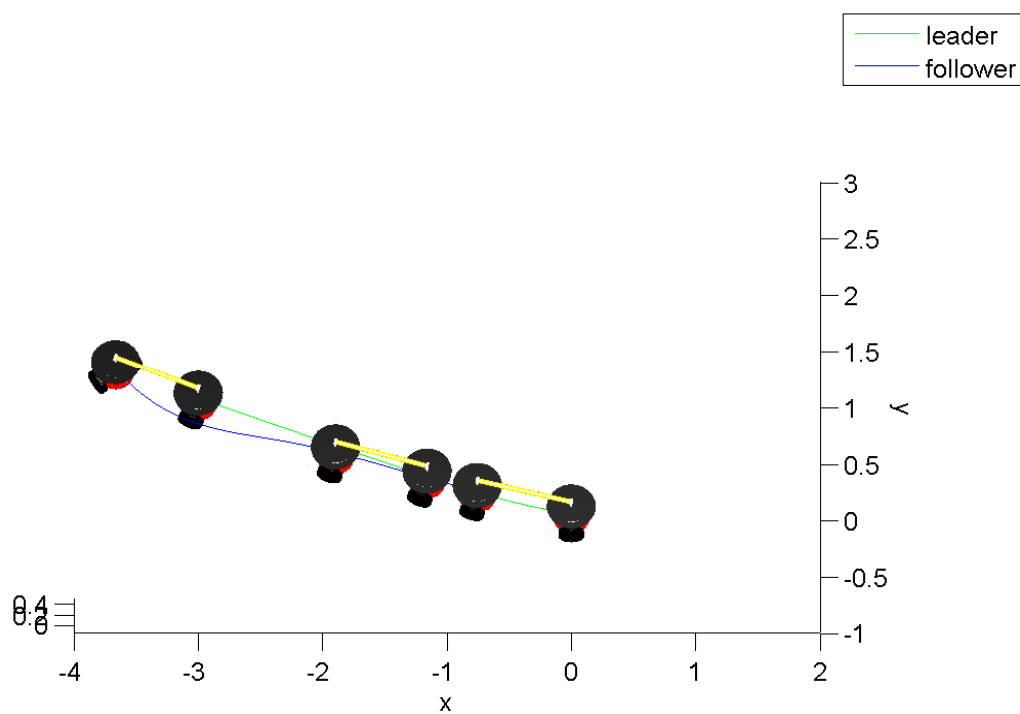


Figure 2.11: Open loop forward motion. Leader converges to the origin with zero heading.

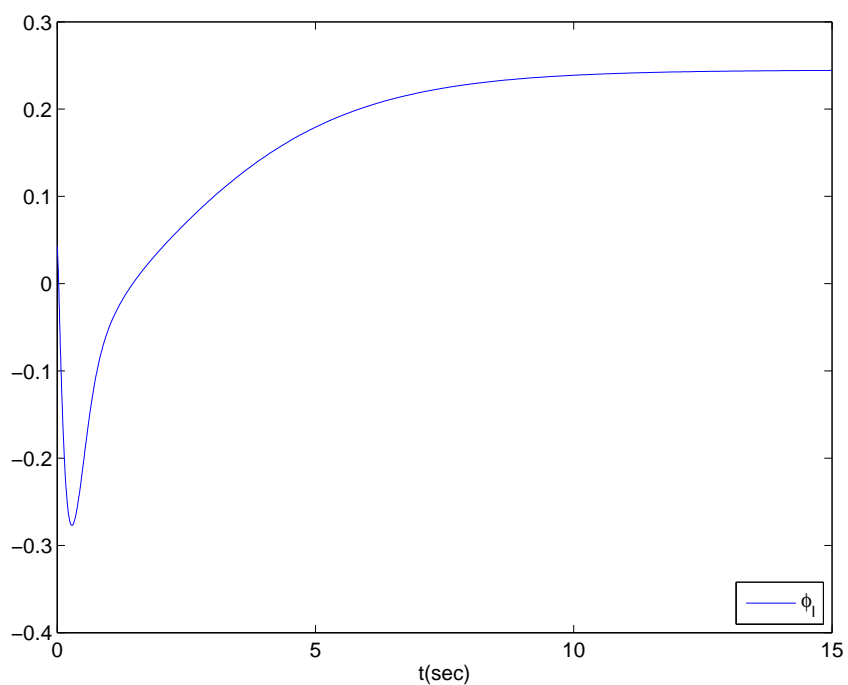


Figure 2.12: Angle ϕ_l may not converge to zero, but at least remains bounded due to large turning radius of the leader.

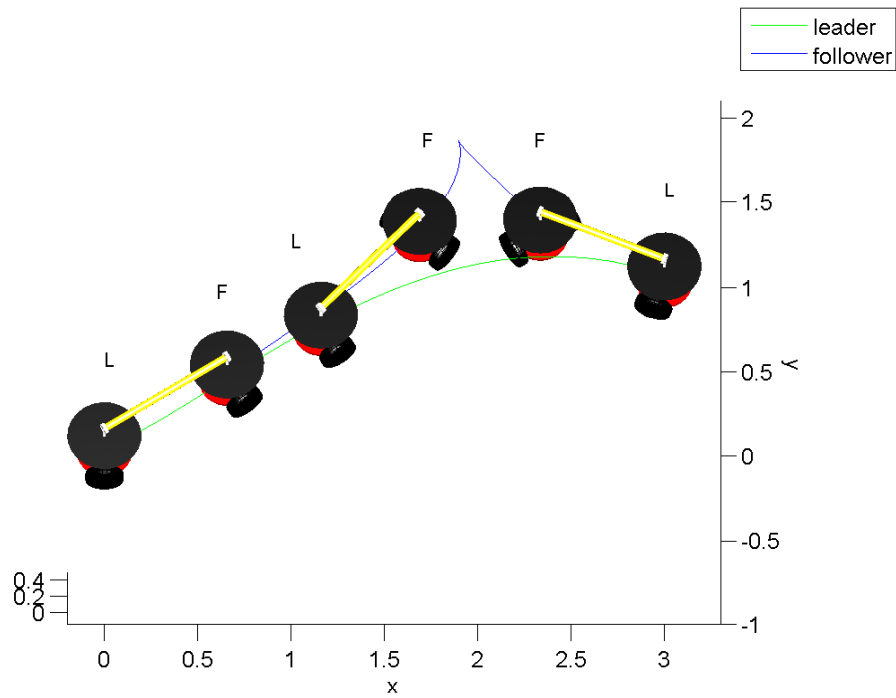


Figure 2.13: Open loop backward motion. Although leader converges to the origin, object heading is reversed.

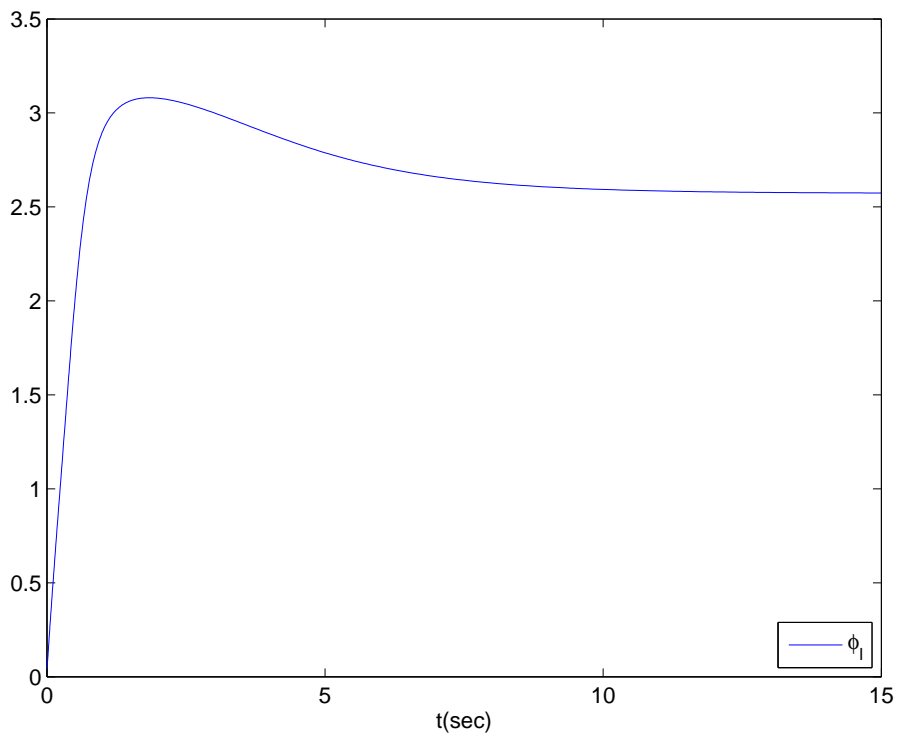


Figure 2.14: Angle ϕ_l is unbounded, it escapes region $(-\frac{\pi}{2}, \frac{\pi}{2})$.

2.3.3 Closed loop scheme

In the previous subsection, it was not possible to stabilize the object's angle without feedback, with backward movement even rendering it unbounded. An approach to overcome backward movement's unboundedness without feedback is a leadership exchange scheme [PPCC02]. However, the only way to effectively overcome the above problems is introducing a feedback law, which uses ϕ_l . In this work we deal with the latter. From now on we consider ϕ_l , and as a result θ , known.

As stated in remark 2.4 and described below, the overall system approximates the nominal model of a car-like robot. In this sense, we can choose a control scheme from the literature and test robustness thereafter. For the point stabilization problem, the aforementioned Astolfi's control law, is adequate. We even prove it renders the system ultimately bounded, with bounds that depend on design and follower's performance. Though, we emphasize that any available control scheme could have been tested instead. Before we deal with this argument formally, we review the nominal car-like model and its conversion to chained form.

Car model

We consider a 4-DOF car-like (fig. 2.15) robot with front-wheel actuation:

$$\begin{aligned} \dot{x} &= u \cos \phi \cos \theta \\ \dot{y} &= u \cos \phi \sin \theta \\ \dot{\theta} &= u \frac{\sin \phi}{l} \\ \dot{\phi} &= r \end{aligned} \tag{2.58}$$

where x, y, θ are the vehicle's coordinates considered on the center of the rear wheels' axis, ϕ is the steering angle, u is the input velocity, r is the steering velocity input and l the distance between front and rear wheels.

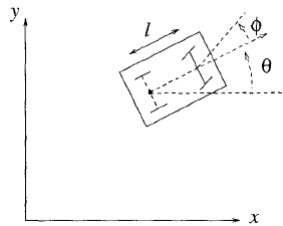


Figure 2.15: Car's model

The above system can be transformed to chained form following local state transformation:

$$\begin{aligned} z_1 &= x \\ z_2 &= \frac{1}{l} \sec^3 \theta \tan \phi \\ z_3 &= \tan \theta \\ z_4 &= y \end{aligned} \tag{2.59}$$

and input change:

$$v_1 = u \cos \phi \cos \theta \quad (2.60)$$

$$v_2 = \left(\frac{3}{l^2} \sec^4 \theta \sin \theta \sin^2 \phi \sec \phi \right) u + \left(\frac{1}{l} \sec^3 \theta \sec^2 \phi \right) r \quad (2.61)$$

the state equations can now be expressed in four dimensional chained form:

$$\begin{aligned} \dot{z}_1 &= v_1 \\ \dot{z}_2 &= v_2 \\ \dot{z}_3 &= z_2 v_1 \\ \dot{z}_4 &= z_3 v_1 \end{aligned} \quad (2.62)$$

To recover the original input signals we use:

$$u = \frac{v_1}{\cos \phi \cos \theta} \quad (2.63)$$

$$r = \left(-\frac{3}{l} \sin^2 \phi \tan \theta \sec \theta \right) v_1 + (l \cos^2 \phi \cos^3 \theta) v_2 \quad (2.64)$$

Perturbed car model

Now we present more rigorously, how our system can be expressed as a perturbed car-like system. In the preceding car equations, coordinates x, y are considered on the rear wheels. In our system, if the follower satisfies the force-torque goals, then, as a side effect, acts like the rear wheels of a car. However, the leader has no access to x_f, y_f to use them in the feedback scheme. To overcome this fact, we resort to estimation of follower's position, considering the point $(x, y) = (x_l, y_l) - L_d (\cos \theta, \sin \theta)$, if measurement of L_d is available. If not we can use L_o , provided the stiffness of the force model is high.

We now express the system's equations with respect to x, y, ϕ_l, θ :

$$\begin{aligned} \dot{x} &= u_l (\cos \phi_l \cos \theta + \epsilon \sin \phi_l \sin \theta) + w \sin \theta \\ \dot{y} &= u_l (\cos \phi_l \sin \theta - \epsilon \sin \phi_l \cos \theta) - w \cos \theta \\ \dot{\theta} &= u_l \frac{\sin \phi_l}{L_d} (1 + \epsilon) + \frac{w}{L_d} \\ \dot{\phi}_l &= r - u_l \epsilon \frac{\sin \phi_l}{L_d} - \frac{w}{L_d} \end{aligned} \quad (2.65)$$

where

$$r = r_l - u_l \frac{\sin \phi_l}{L_o} \quad (2.66)$$

is the perturbed system's steering velocity and

$$\epsilon = \frac{L_d}{L} - 1 \quad (2.67)$$

$$w = u_f \frac{L_d}{L} \sin \phi_f \quad (2.68)$$

are the disturbances, caused by the estimation error and follower's misalignment respectively.

Respectively, we can transform (2.65) into a perturbed chained form. Applying transformation (2.59) and assuming $\theta, \phi_l \in (-\frac{\pi}{2}, \frac{\pi}{2})$ we acquire:

$$\begin{aligned}
\dot{z}_1 &= \left(1 + \epsilon L_d \frac{z_2 z_3}{(1 + z_3^2)^{\frac{3}{2}}} \right) v_1 + w \frac{z_3}{\sqrt{1 + z_3^2}} \\
\dot{z}_2 &= v_2 + \epsilon \frac{v_1}{L_d^2} \left(3L_d^2 \frac{z_2^2 z_3}{1 + z_3^2} - L_d z_2 (1 + z_3^2)^{\frac{1}{2}} - L_d^3 \frac{z_2^3}{(1 + z_3^2)^{\frac{5}{2}}} \right) \\
&\quad + w \frac{1}{L_d^2} \left(3L_d z_2 z_3 - (1 + z_3^2)^{\frac{3}{2}} - L_d^2 \frac{z_2^2}{(1 + z_3^2)^{\frac{3}{2}}} \right) \\
\dot{z}_3 &= (1 + \epsilon) z_2 v_1 + w \frac{1 + z_3^2}{L_d} \\
\dot{z}_4 &= \left(z_3 - \epsilon \frac{L_d z_2}{(1 + z_3^2)^{\frac{3}{2}}} \right) v_1 - w \frac{1}{\sqrt{1 + z_3^2}}
\end{aligned} \tag{2.69}$$

Observe that the above system is a perturbed version of (2.62).

Control

Putting control inputs (2.51), and using transformation 2.49 we obtain:

$$\begin{aligned}
\dot{z}_1 &= -kz_1 + k\epsilon g_{11}(z_1, \xi) + w g_{12}(z_1, \xi) \\
\dot{\xi}_2 &= p_2 \xi_2 + p_3 \xi_3 + p_4 \xi_4 + k\epsilon g_{21}(z_1, \xi) + w g_{22}(z_1, \xi) \\
\dot{\xi}_3 &= -k\xi_2 + k\xi_3 + k\epsilon g_{31}(z_1, \xi) + w g_{32}(z_1, \xi) \\
\dot{\xi}_4 &= -k\xi_3 + 2k\xi_4 + k\epsilon g_{41}(z_1, \xi) + w g_{42}(z_1, \xi)
\end{aligned} \tag{2.70}$$

where functions g_{ij} are the nonlinear perturbation's terms:

$$\begin{aligned}
g_{11} &= -L_d \frac{z_1^2 \xi_2 \xi_3}{(1 + z_1^2 \xi_3^2)^{\frac{3}{2}}} \\
g_{12} &= \frac{z_1 \xi_3}{\sqrt{1 + z_1^2 \xi_3^2}} \\
g_{21} &= z_1 \left(-3 \frac{z_1 \xi_2^2 \xi_3}{1 + z_1^2 \xi_3^2} + \frac{1}{L_d} \xi_2 (1 + z_1^2 \xi_3^2)^{\frac{1}{2}} + L_d \frac{\xi_2^3}{(1 + z_1^2 \xi_3^2)^{\frac{5}{2}}} \right) \\
g_{22} &= \frac{1}{L_d^2} \left(3L_d z_1 \xi_2 \xi_3 - (1 + z_1^2 \xi_3^2)^{\frac{3}{2}} - L_d^2 \frac{\xi_2^2}{(1 + z_1^2 \xi_3^2)^{\frac{3}{2}}} \right)
\end{aligned}$$

$$\begin{aligned}
g_{31} &= -\xi_2 + L_d \frac{z_1 \xi_2 \xi_3^2}{(1 + z_1^2 \xi_3^2)^{\frac{3}{2}}} \\
g_{32} &= \frac{1 + z_1^2 \xi_3^2}{L_d z_1} - \frac{\xi_3^2}{\sqrt{1 + z_1^2 \xi_3^2}} \\
g_{41} &= 2L_d \frac{z_1 \xi_2 \xi_3 \xi_4}{(1 + z_1^2 \xi_3^2)^{\frac{3}{2}}} + L_d \frac{\xi_2}{z_1 (1 + z_1^2 \xi_3^2)^{\frac{3}{2}}} \\
g_{42} &= -2 \frac{\xi_3 \xi_4}{\sqrt{1 + z_1^2 \xi_3^2}} - \frac{1}{z_1^2 \sqrt{1 + z_1^2 \xi_3^2}}
\end{aligned} \tag{2.71}$$

Notice that perturbation is nonvanishing. Whereas, asymptotic stability cannot be achieved, accomplishing ultimate boundedness is possible, provided we prevent z_1 from becoming too small. Functions g_{ij} are bounded if (z_1, ξ) lie within a set $D^+ = (\underline{z}, r_1) \times \{\xi : |\xi| < r\}$ or $D^- = (-r_1, -\underline{z}) \times \{\xi : |\xi| < r\}$, where \underline{z} is the smallest allowed value of $|z_1|$. The lower bound imposed on $|z_1|$, is due to some of the g_{ij} functions having a z_1 term in the denominator, thus being unbounded in a set containing the origin.

With proper gains and sufficiently small $|w|, |\epsilon|$ steady-state errors system (2.70) can reach an desired ultimate bound. However, when z_1 reaches its lower bound the system must stop (zero inputs), since perturbation becomes unbounded.

We summarize the above in the control law:

$$v = \begin{cases} \text{control law (2.51) if } |z_1| > b_1 > \underline{z} \\ [0 \ 0]^T \text{ if } |z_1| \leq b_1 \end{cases} \tag{2.72}$$

where b_1 is the desired bound on z_1 . In the following subsection we prove that the above control law renders the system (2.65) locally ultimately bounded with desired bounds, provided errors $|\epsilon|, |w|$ are small enough and gains k, p_i are chosen properly.

2.3.4 Closed loop scheme robustness analysis

System (2.70) can be also written in the following way:

$$\dot{z}_1 = -kz_1 + g_1(t, z_1, \xi) \tag{2.73}$$

$$\dot{\xi} = A\xi + g(t, z_1, \xi) \tag{2.74}$$

Functions g_{ij}, g_i are bounded and smooth if (z_1, ξ) lie within a set $D^+ = (\underline{z}, r_1) \times B_r$ or $D^- = (-r_1, -\underline{z}) \times B_r$, where $B_r = \{\xi : |\xi| < r\}$ Furthermore:

$$A = \begin{bmatrix} p_2 & p_3 & p_4 \\ -k & k & 0 \\ 0 & -k & 2k \end{bmatrix}$$

with p_i we place eigenvalues at desired positions. We can write:

$$A = U\Lambda U^{-1} \tag{2.75}$$

with

$$\Lambda = \begin{bmatrix} -\lambda_1 & 0 & 0 \\ 0 & -\lambda_2 & 0 \\ 0 & 0 & -\lambda_3 \end{bmatrix} \quad (2.76)$$

$$U = [u_1 \quad u_2 \quad u_3] \quad (2.77)$$

the matrix containing the normalized eigenvectors of A .

The following lemma proves that if the initial values lie within a region of attraction, then state begins to exponentially decrease, until some bounds are reached or system escapes D^+ (or D^-) due to $|z_1|$ becoming smaller than \underline{z} . If we also manage to tune convergence rates (Corollary 2.1) we can ensure that bounds are reached before the solution escapes D^+ (or D^-).

Lemma 2.2. *Consider system (2.73)-(2.74). Suppose the perturbation terms satisfy:*

$$|g_1(t, z_1, \xi)| \leq \delta_1 < k\mu_1 r_1 \quad (2.78)$$

$$|U^{-1}| |g(t, z_1, \xi)| \leq \delta < \lambda_{\min} \sqrt{\frac{\lambda_{\min}}{\lambda_{\max}}} \mu \frac{r}{|U|} \quad (2.79)$$

for all $t \geq 0$, all $(z_1, \xi) \in D^+, D^-$, and some positive constants $\mu_1 < 1$, $\mu < 1$. Also suppose $\underline{z} < \frac{\delta_1}{k\mu_1}$. Then for all $|z_1(0)| < r_1$, $|z_1(0)| > \frac{\delta_1}{k\mu_1}$, $|\xi(0)| < \frac{1}{|U^{-1}|} \sqrt{\frac{\lambda_{\min}}{\lambda_{\max}}} \frac{r}{|U|}$, the solutions of the perturbed systems satisfy:

$$|z_1(t)| \leq \exp[-\gamma_1 t] |z_1(0)|, \forall t < T_1 \quad (2.80)$$

$$|z_1(t)| \leq b_1, \forall t \geq T_1, t < t_{\max} \quad (2.81)$$

$$|\xi(t)| \leq |U| k_\xi \exp[-\gamma t] |U^{-1}| |\xi(0)|, \forall t < \min\{T, t_{\max}\} \quad (2.82)$$

$$|\xi(t)| \leq |U| b, \forall t \geq T, t < t_{\max} \text{ if } T < t_{\max} \quad (2.83)$$

for finite T_1, T , where:

$$\gamma_1 = k(1 - \mu_1), b_1 = \frac{1}{k} \frac{\delta_1}{\mu_1}$$

$$k_\xi = \sqrt{\frac{\lambda_{\max}}{\lambda_{\min}}}, \gamma = \lambda_{\min}(1 - \mu), b = \frac{1}{\lambda_{\min}} \sqrt{\frac{\lambda_{\max}}{\lambda_{\min}}} \frac{\delta}{\mu}$$

t_{\max} is such that a maximal solution $(z_1(t), \xi(t))$ on the interval $[0, t_{\max})$ exists. If $z_1(0) > 0$ then $(z_1(t), \xi(t)) \in D^+, \forall t \in [0, t_{\max})$. If $z_1(0) < 0$ we replace D^+ with D^- .

Proof. Without loss of generality we suppose $z_1(0) > 0$ (the steps are the same in the negative case).

Phase A: Existence of maximal solution. Set D^+ is nonempty and open. Moreover, owing to assumptions $(z_1(0), \xi(0)) \in D^+$. Additionally, due to the smoothness of the disturbances and the proposed control scheme, over D^+ , it can be easily verified that right side of system (2.70) is continuous on t and continuous for all $(z_1(t), \xi(t)) \in D^+$. Therefore, the hypotheses of Theorem B.1 stated in Appendix

B hold and the existence of a maximal solution $\xi(t)$ of (2.32) on a time interval $[0, t_{\max})$ such that $(z_1(t), \xi(t)) \in D^+$, $\forall t \in [0, t_{\max})$ is ensured.

Phase B: Region of attraction and bounds of ξ . Consider similarity transformation $\hat{\xi} = U^{-1}\xi$. Then system (2.74) becomes:

$$\dot{\hat{\xi}} = \Lambda \hat{\xi} + U^{-1} \tilde{g}(t, z_1, \hat{\xi}) \quad (2.84)$$

where $\tilde{g}(t, z_1, \hat{\xi}) = g(t, z_1, U\hat{\xi})$.

Now we define $\tilde{B}_r = \{\hat{\xi} : |\hat{\xi}| < \frac{r}{|U|}\}$. If $\hat{\xi} \in \tilde{B}_r$ then since $|\xi| \leq |U||\hat{\xi}|$, also $\xi \in B_r$ and as a result $\max_{\hat{\xi} \in \tilde{B}_r} |\tilde{g}(t, z_1, \hat{\xi})| \leq \max_{\xi \in B_r} |g(t, z_1, \xi)|$. If inequality (2.79) is satisfied then also:

$$|U^{-1}| |\tilde{g}(t, z_1, \hat{\xi})| \leq \delta < \lambda_{\min} \sqrt{\frac{\lambda_{\min}}{\lambda_{\max}}} \mu \frac{r}{|U|} \quad (2.85)$$

Moreover Lyapunov function:

$$V = -\frac{1}{2} \hat{\xi}^T \Lambda^{-1} \hat{\xi} \quad (2.86)$$

satisfies:

$$\begin{aligned} \frac{1}{2\lambda_{\max}} |\hat{\xi}|^2 &\leq V \leq \frac{1}{2\lambda_{\min}} |\hat{\xi}|^2 \\ \frac{\partial V}{\partial \hat{\xi}} \Lambda \hat{\xi} &= -|\hat{\xi}|^2 \\ \left| \frac{\partial V}{\partial \hat{\xi}} \right| &\leq \frac{1}{\lambda_{\min}} |\hat{\xi}| \end{aligned} \quad (2.87)$$

Differentiating V we obtain:

$$\begin{aligned} \dot{V} &\leq -|\hat{\xi}|^2 + \frac{\delta}{\lambda_{\min}} |\hat{\xi}| \\ &= -(1-\mu) |\hat{\xi}|^2 - \mu |\hat{\xi}|^2 + \frac{\delta}{\lambda_{\min}} |\hat{\xi}| \\ &\leq -(1-\mu) |\hat{\xi}|^2, \forall |\hat{\xi}| \geq \frac{\delta}{\lambda_{\min} \mu} \\ &\leq -2\lambda_{\min} (1-\mu) V, \forall |\hat{\xi}| \geq \frac{\delta}{\lambda_{\min} \mu} \end{aligned}$$

Any Lyapunov surface $\Omega_c = \{\hat{\xi} : V(\hat{\xi}) \leq c\}$ that contains ball $\tilde{B}_{|U|\delta/\lambda_{\min}\mu}$ and is a subset of \tilde{B}_r is positive invariant for state ξ on the interval $[0, t_{\max})$. Such a surface exists if $\tilde{B}_r \supset \Omega_c \supseteq \tilde{B}_{|U|\delta/\lambda_{\min}\mu}$ for some c . The first set relation holds if c satisfies $c < \bar{c} = \min_{\tilde{B}_r} V = \frac{1}{2\lambda_{\max}} \left(\frac{r}{|U|}\right)^2$. The second holds for $c \geq \underline{c} = \max_{\tilde{B}_{|U|\delta/\lambda_{\min}\mu}} V = \frac{1}{2\lambda_{\min}} \left(\frac{\delta}{\lambda_{\min}\mu}\right)^2$. From condition (2.85) $\bar{c} > \underline{c}$ and as a result, such surfaces Ω_c exist $\forall c \in [\underline{c}, \bar{c})$. The smallest invariant set from the above analysis is $\Omega_{\underline{c}}$. The ultimate

bound is the smallest ball that includes $\Omega_{\underline{c}}$, which is $|\hat{\xi}| < b$. With similar analysis we deduce that the initial state must lie inside the largest ball included in $\Omega_{\bar{c}}$, namely $|\hat{\xi}| < \sqrt{\frac{\lambda_{min}}{\lambda_{max}}} \frac{r}{|U|}$.

Now if we apply the comparison lemma B.1 to the above inequality we acquire:

$$V \leq \exp[-2\gamma t] V(0), t \in [0, t_{max}]$$

or

$$\begin{cases} V \leq \exp[-2\gamma t] V(0), t \in [0, T] & \text{if } T < t_{max} \\ V \leq \underline{c}, t \in [T, t_{max}] \end{cases}$$

Using $|\xi| \leq |U| |\hat{\xi}|$, $|\hat{\xi}| \leq |U^{-1}| |\xi|$ and $\frac{1}{2\lambda_{max}} |\hat{\xi}|^2 \leq V \leq \frac{1}{2\lambda_{min}} |\hat{\xi}|^2$ we prove (2.82)-(2.83).

Phase C: Region of attraction and bounds of z_1 . If the solution escapes D^+ then it escapes from surface $|z_1| = \underline{z}$

Consider now Lyapunov function $V_1 = \frac{1}{2} z_1^2$. Differentiating we obtain:

$$\begin{aligned} \dot{V}_1 &\leq -k |z_1|^2 + \delta_1 |z_1| \\ &\leq -(1 - \mu_1) k |z_1|^2, \forall |z_1| \geq \frac{\delta_1}{k\mu_1} \\ &\leq -2(1 - \mu_1) k V_1, \forall |z_1| \geq \frac{\delta_1}{k\mu_1} \end{aligned}$$

Again, applying the comparison lemma B.1 we obtain:

$$V_1 \leq \exp[-2\gamma_1 t] V_1(0), t \in [0, t_{max}]$$

or

$$\begin{cases} V_1 \leq \exp[-2\gamma_1 t] V_1(0), t \in [0, T_1] & \text{if } T_1 < t_{max} \\ V_1 \leq \frac{1}{2} b_1^2, t \in [T_1, t_{max}] \end{cases}$$

We will prove that the first case never occurs. If initial conditions are satisfied V, V_1 are decreasing and $z_1(t) \leq z_1(0) < r_1$, $|\xi| \leq |U| k_\xi |U^{-1}| |\xi(0)| < r$, $\forall t \in [0, t_{max}]$. Suppose z_1 never reaches b_1 before t_{max} . Then also $z_1 > b_1 > \underline{z}$. As a result, state never escapes the compact subset $[b_1, z_1(0)] \times \{\xi : |\xi| \leq |U| k_\xi |U^{-1}| |\xi(0)|\} \subset D^+$. Following the same steps as in the proof of theorem 2.1 we must replace t_{max} with ∞ (contradiction with Proposition B.1). However, since we assumed $T_1 > t_{max}$ and T_1 is finite this leads to contradiction. Thus, only the second case occurs.

Finally, using $z_1 = \sqrt{2V_1}$ we prove (2.80)-(2.81). \square

Remark 2.12. *We can always achieve $b_1 > \underline{z}$ since disturbances $|\epsilon|, |w|$ can be made arbitrarily small and compensate an increase in $|g|$.*

Remark 2.13. *Bounds b_1, b can be adjusted, provided $|\epsilon|, |w|$ are chosen small enough.*

Remark 2.14. *Boundaries r, r_1 and, as a result, the initial regions, can be adjusted, provided $|\epsilon|, |w|$ are chosen small enough.*

Remark 2.15. *The above specifications for ϵ , w can be achieved at steady state. Using a small time constant in the prescribed functions, convergence is made fast enough, that conditions of the above lemma are not violated.*

Corollary 2.1. *If conditions of previous lemma are met and:*

$$\ln \left(\frac{|\xi(0)| |U^{-1}| k_\xi}{b} \right)^{\frac{1}{\gamma}} < \ln \left(\frac{|z_1(0)| + \delta_1}{b_1 + \delta_1} \right)^{\frac{1}{k}}$$

then $T < T_1 < t_{max}$ and ξ reaches its bound before z_1 .

Proof. From (2.82) putting $|\xi| = |U|b$, we obtain $T \leq \ln \left(\frac{(\xi(0)|U^{-1}|k_\xi)}{b} \right)^{\frac{1}{\gamma}}$. Suppose again without loss of generality that $z_1(0) > 0$. From (2.73) the fastest possible decreasing solution is:

$$z_{1fast}(t) = -\frac{\delta_1}{k} + \left(\frac{z_1(0) + \delta_1}{k} \right) \exp[-kt], \forall t \in [0, t_{max}] \quad (2.88)$$

If we put b_1 to the above equation $T_1 \geq \ln \left(\frac{|z_1(0)| + \delta_1}{b_1 + \delta_1} \right)^{\frac{1}{k}}$ and the proof is completed. \square

Remark 2.16. *The most influencing factor to satisfy the above inequality is choice of eigenvalues λ_i and gain k . We must choose $\lambda_i > k$.*

Corollary 2.2. *If conditions of lemma and previous corollary are met then under control law (2.72) with switching taking place at T_1 , system (2.65) is ultimately bounded.*

When control $[u_l \ r_l]^T = [0 \ 0]^T$ is applied it is easy to show from eq. (2.36) that $w \rightarrow 0$. As a result, disturbance w in eq. (2.65) is not high enough to drive system away from the ultimate bounds.

Remark 2.17. *The bounds on the original chained form coordinates z_3, z_4 have multiplicative effect since $|z_3| = |\xi_3| |z_1| \leq |U| b b_1$, $|z_4| = |\xi_3| |z_1|^2 \leq |U| b b_1^2$. Therefore even if corollary 2.1 does not hold $z_{3,4}$ are sufficiently bounded. It is not important to achieve a low bound for z_2 . This state variable can be stabilized even after the task is completed with $u_l = 0$.*

Remark 2.18. *If $|z_1(0)| < b_1$ then we can either readjust bound b_1 properly or just open loop control the system away from the origin.*

2.3.5 Closed loop scheme simulation

We demonstrate the overall system's performance under the closed loop law. We test both movement directions with various initial postures. Goal configuration of the perturbed car-like system is the origin, with zero heading and steering angle. We choose bounds $b_1 = 0.01$, $b = 0.1$ (although the theoretical analysis

could more conservative these bounds work in practice), gain $k = 0.2$ and all eigenvalues $\lambda_i = 0.5$. Follower's performance functions are $\rho_f = (50 - 0.1)e^{-2t} + 0.1$, $\rho_\tau = (30 - 0.1)e^{-2t} + 0.1$. The rest of follower's specifications are the same as with the open loop scheme. Figure 2.16 shows the trajectory of the system, in forward motion with negative initial angle θ . Figure 2.17 displays the respective evolution of the state variables. We notice that states y , θ , ϕ_i converge faster than x since the eigenvalues λ_i are chosen larger than k . Of course, unlike the open loop scheme θ converges to a small neighbourhood of 0.

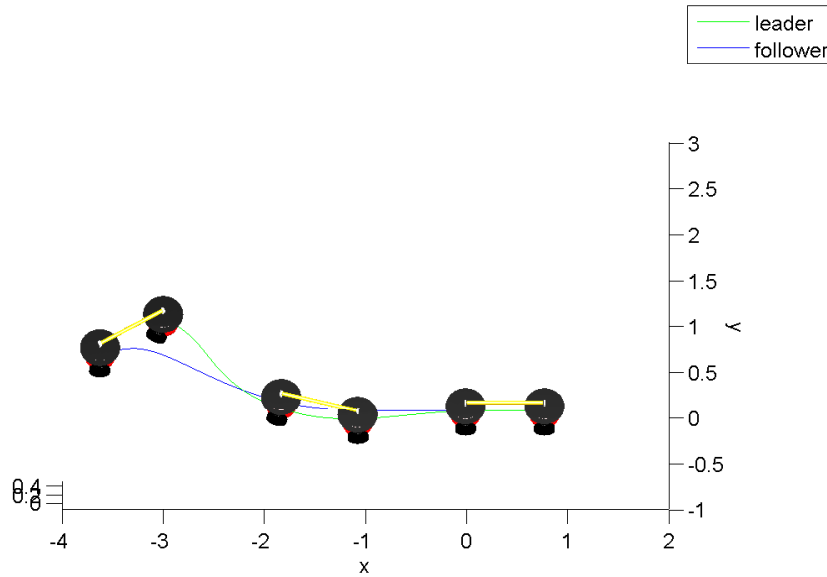


Figure 2.16: Forward motion for positive initial θ

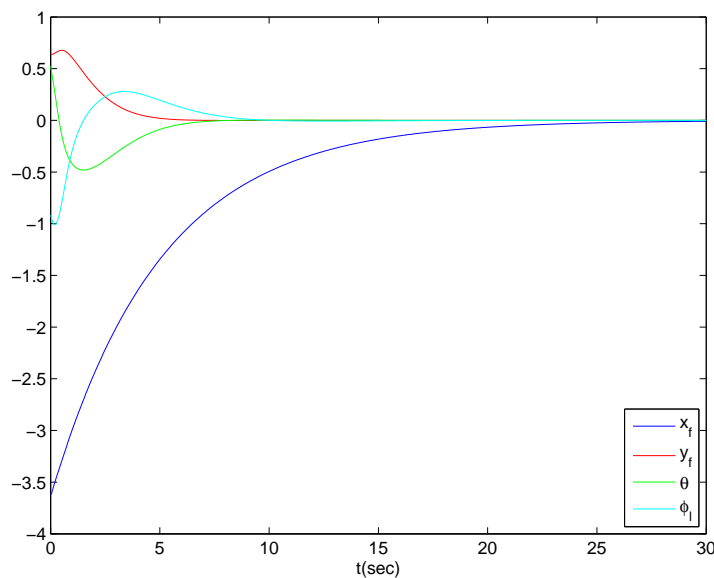


Figure 2.17: Evolution of state

For completeness we also include the following figures 2.18-2.19, which display the evolution of state in chained form and in form 2.49.

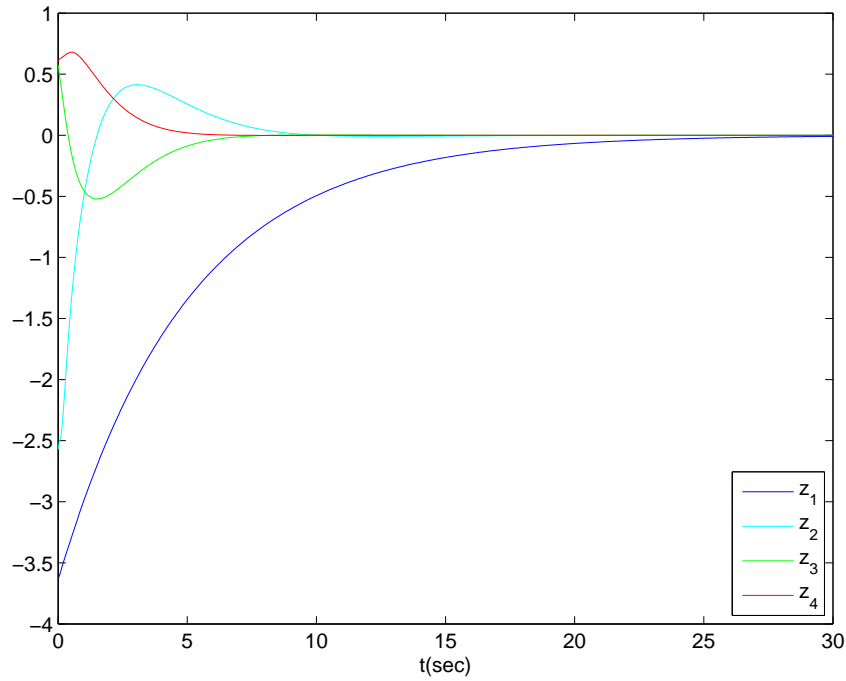


Figure 2.18: Evolution of state in chained form

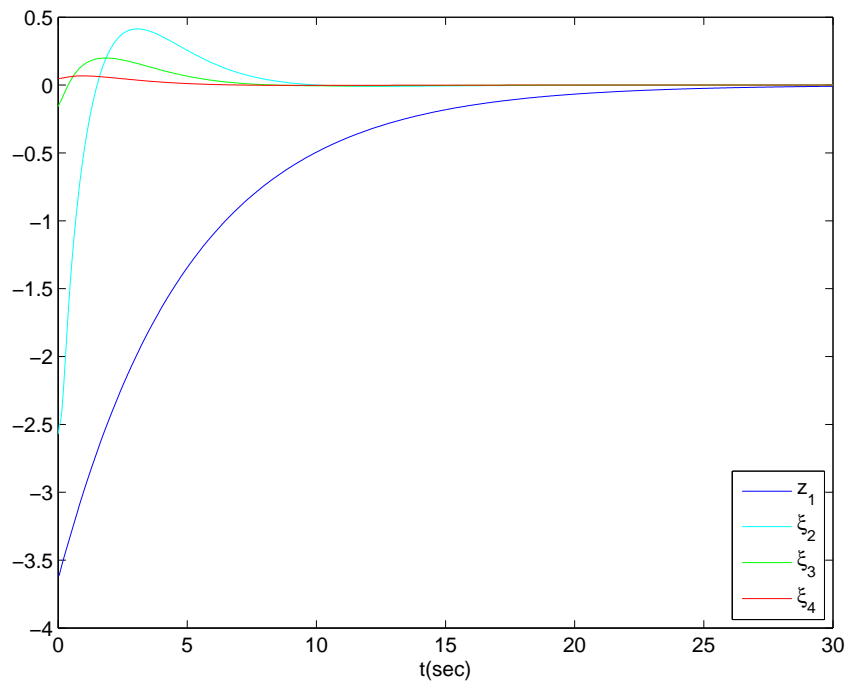


Figure 2.19: Evolution of state in form 2.49

Now we present results for backward motion. Figure 2.20 depicts system's trajectory for positive initial θ angle. Figure 2.21 demonstrates closed loop scheme's importance. We compare ϕ_l 's behaviour for both schemes. Notice that the unboundedness problem is completely solved.

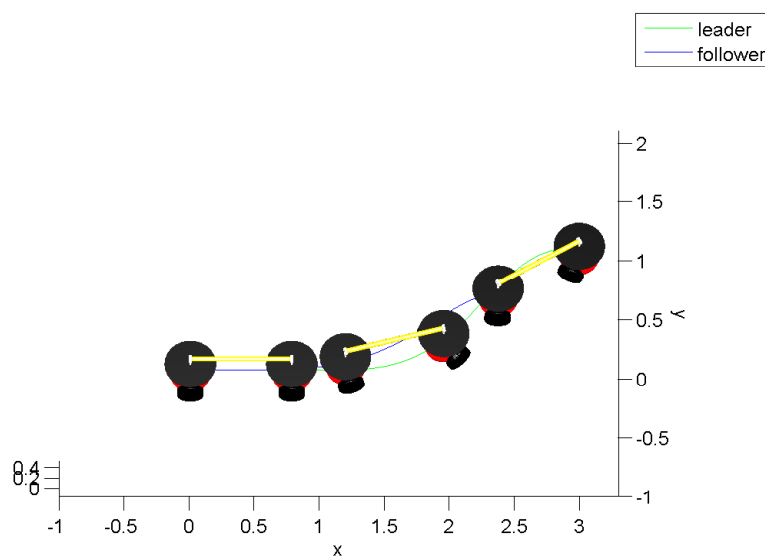


Figure 2.20: Backward motion for positive initial θ

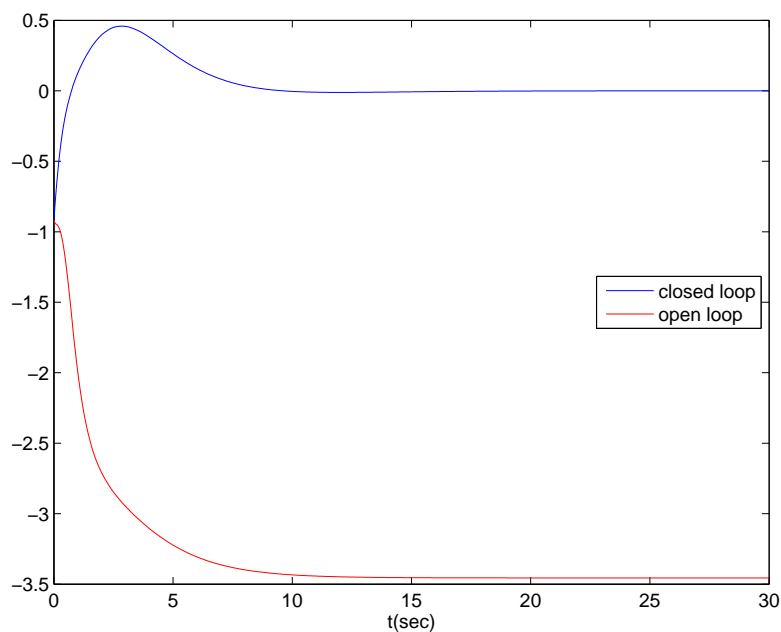


Figure 2.21: Behaviour of angle ϕ_l in the closed and open loop case, during backward motion. Of course, the former scheme manages to overcome the unboundedness problems caused by the latter.

Finally, in figures 2.22-2.23 we present trajectories for negative initial θ angles.

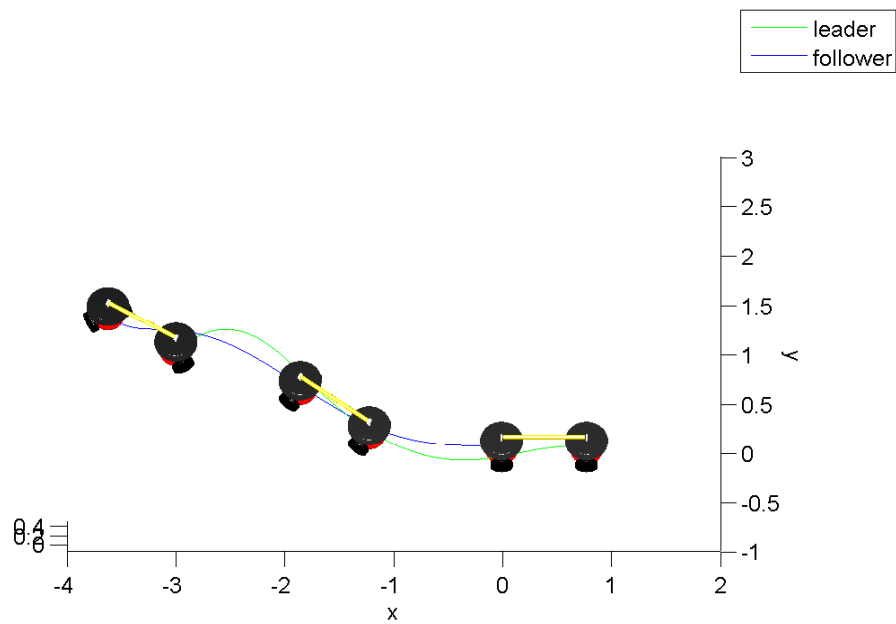


Figure 2.22: Forward motion for negative initial θ

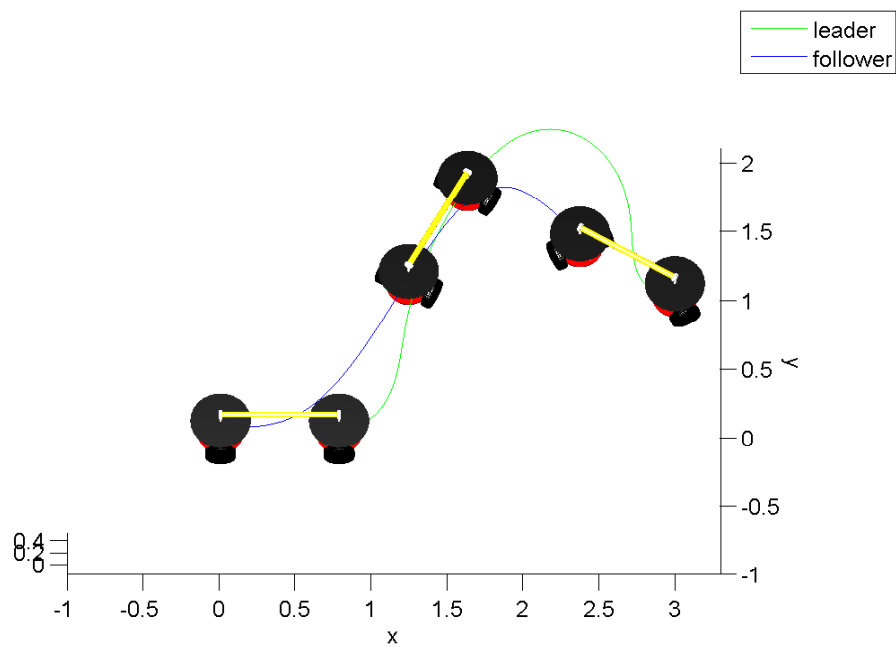


Figure 2.23: Backward motion for negative initial θ

Chapter 3

Cooperation of mobile manipulators

This chapter examines the second cooperative scenario. Instead of nonholonomic mobile robots, the team now consists of two holonomic mobile manipulators (fig. 3.1). Again, the formation is of leader-follower type. There is generally no restriction on the shape of the object and its motion can have all six degrees of freedom. It is assumed that the robots have at least 6-DOFs (Degrees Of Freedom), although redundancy is preferred. Since, this formation has enough mobility, compliant contacts and free revolute joints are no longer needed. Contact between the robot and the object is considered rigid, thus force and torque are introduced exclusively in the dynamic model. Certainly, this architecture is more symmetric than the one presented in the previous chapter.



Figure 3.1: Cooperation of mobile manipulators

The main goal of the leader is to achieve a desired trajectory profile for the object, via imposing an impedance law control. This profile does not need to be known before task execution and can even be generated on-line (i.e. using a potential field). The follower tries to estimate leader's desired motion and imposes an impedance law using the estimated signals instead of the desired. Both impedance laws are imposed after feedback linearization. Due to the rigid link that is formed via the object between the two end-effectors, and the fact that the same impedance time constants are used, we can design an estimation law, which drives the estimation error to an arbitrarily small residual set. Furthermore, load sharing is achieved, by choosing proper impedance parameters, and excessive forces are avoided. Notice that not only the architecture, but also the objectives are more symmetric.

We point out that no explicit communication is used. Both agents use only their own force, position and velocity measurements. The only information needed, is few parameters, which can be transmitted off-line from the leader to the follower.

Moreover, the geometric and inertial parameters of each robot is considered known to itself, while object's parameters are known to all. Finally, both robots have a common coordinate system.

This chapter mainly follows the analysis of a series of papers published by Kotsuge et. al. [KO96], [KOC97], [KOS97]. We extend their work, by modifying the estimation law, to make it more robust, by including the object's mass in the system model and finally by introducing load sharing coefficients.

To conclude this introduction we present the chapter's structure:

- System model derivation. The model of each separate agent is presented, followed by object's model.
- Control law.
- Follower's estimation law.
- Simulation.

3.1 System Model

The derivation of the system's kinematics is based on the Denavit–Hartenberg convention. Respectively, we use the Euler-Lagrange formulation for the dynamic model. For a good introduction on both topics, refer to [SSVO09].

Since the mobile base is holonomic, its degrees of freedom are treated like two prismatic and a revolute joint. The manipulator consists of revolute joints, with the overall robot having six or more DOF's in total. Naturally, if the mobile manipulator has redundant DOF's, they can be utilized for accomplishing secondary objectives, such as obstacle avoidance or maximization of manipulability.

As shown in figure 3.2 the multi-effector/object system is a closed kinematic chain, consisting of the follower, the leader and the object. Since the contacts are rigid, constraint $\|p_o - p_i\| = \|l_i\| = \text{const}$, $i \in \{f, l\}$ is in effect, where p_i are the task space variables and p_o the object's variables with respect to an inertial frame

$\{I\}$. Thus, the DOFs of the overall system are less than the addition of the separate DOFs of each system ([Kha88]).

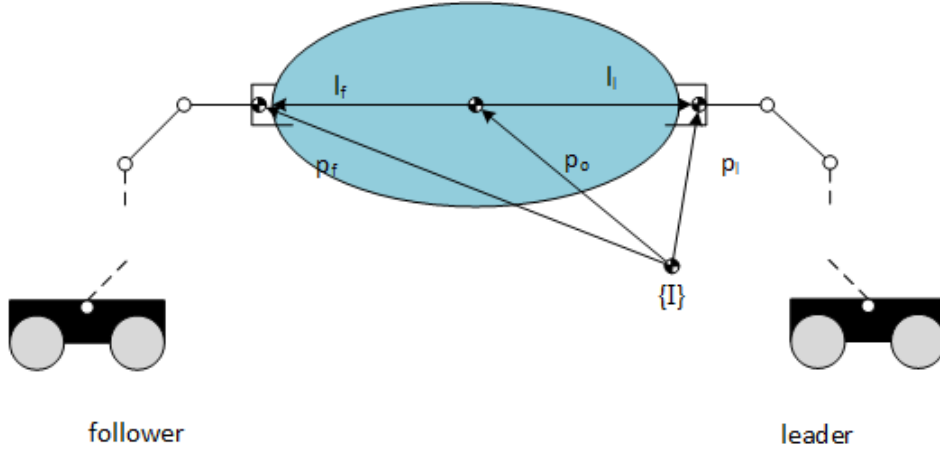


Figure 3.2: Multi-effector/object system

3.1.1 Kinematics

Let q_i , $i \in \{f, l\}$ be the joint space variables. If we express each robot's equations in task space we obtain:

$$\begin{aligned} p_i &= f(q_i) \\ \dot{p}_i &= J(q_i) \dot{q}_i \end{aligned} \quad (3.1)$$

The location of a rigid body $p_i = [r_i^T, \phi_i^T]^T$ contains vectors r_i , ϕ_i , which define its position and orientation respectively. Since geometric parameters l_i are considered known to each robot i , the object's position can be computed from the following equation:

$$p_o = p_i - l_i \quad (3.2)$$

Differentiating the above we obtain:

$$\begin{aligned} \dot{r}_i &= \dot{r}_o + \dot{\phi}_i \times l_o \\ \dot{\phi}_i &= \dot{\phi}_o \end{aligned}$$

or in matrix form:

$$\dot{p}_i = J_{oi} \dot{p}_o = \begin{bmatrix} I_{3 \times 3} & -L_i \\ 0_{3 \times 3} & I_{3 \times 3} \end{bmatrix} \dot{p}_o \quad (3.3)$$

where J_{oi} is the Jacobian from the end-effector to the object's center of mass and

$$L_i = \begin{bmatrix} 0 & -l_{iz} & l_{iy} \\ l_{iz} & 0 & -l_{ix} \\ -l_{iy} & l_{ix} & 0 \end{bmatrix}$$

the cross-product matrix. Notice that since the end-effector and the object are rigidly connected, this Jacobian has always full rank and inverse J_{oi}^{-1} . Finally, differentiating again we gain an acceleration relation:

$$\ddot{p}_i = \dot{J}_{oi} \dot{p}_o + J_{oi} \ddot{p}_o \quad (3.4)$$

3.1.2 Dynamics

The dynamic model in terms of task space variables, for a single robot, is described by:

$$M_i(q_i)\ddot{p}_i + C_i(\dot{q}_i, q_i)\dot{p}_i + G_i(q_i) = U_i + F_i, \quad i \in \{f, l\} \quad (3.5)$$

where M_i is the positive definite inertial matrix, C_i is a matrix representing Coriolis and centrifugal forces and G_i represents gravitational forces. F_i is the force exerted on the robot by the object and U_i are the task space forces. The relation between input torques τ_i and the task space forces is:

$$\tau_i = J_i^T U_i + \left(I - J_i^T \bar{J}_i^T \right) \tau_{in} \quad (3.6)$$

where \bar{J}_i is the generalized inverse that is consistent with the equations of motion of the manipulator and its end-effector [Kha88]. The vector τ_{in} does not contribute to the end-effector's forces since it is projected in the null space of \bar{J}_i . This relation provides a decomposition of joint forces into two dynamically decoupled control vectors: joint forces corresponding to forces acting at the end effector ($J_i^T U_i$) and joint forces that only affect internal motions $\left(\left[I - J_i^T \bar{J}_i^T \right] \tau_{in} \right)$. These internal forces can be regulated independently to achieve secondary goals, while the end-effector is controlled by the desired task space forces.

Using the kinematic relations (3.2)-(3.4), we can express the above dynamic model, with respect to object's variables:

$$M_{oi}(q_i)\ddot{p}_o + C_{oi}(\dot{q}_i, q_i)\dot{p}_o + G_{oi}(q_i) = J_{oi}^T U_i + J_{oi}^T F_i \quad (3.7)$$

where $M_{oi}(q_i) = J_{oi}^T M_i(q_i) J_{oi}$, $C_{oi}(\dot{q}_i, q_i) = J_{oi}^T (C_i(\dot{q}_i, q_i) J_i + M_i(q_i) \dot{J}_i)$ and $G_{oi}(q_i) = J_{oi}^T G_i(q_i)$.

The dynamics equation of the object is given by

$$M_o(p_o)\ddot{p}_o + C_o(\dot{p}_o, p_o)\dot{p}_o + G_o(p_o) = -J_{ol}^T F_l - J_{of}^T F_f \quad (3.8)$$

where, we assume that no external forces are exerted on the object.

Finally, the grasp model is presented. Total force exerted on the object is equal to $F_o = -J_{ol}^T F_l - J_{of}^T F_f = -GF$, where

$$G = \begin{bmatrix} J_{ol}^T & J_{of}^T \end{bmatrix} \quad (3.9)$$

is the grasp matrix of the overall configuration and $F = \begin{bmatrix} F_l \\ F_f \end{bmatrix}$. Forces projected on the null space of G do not contribute to the object force. Therefore, we can use component $F_{int} = (I - G^\# G) \hat{F}_{int}$ to regulate the steady-state internal forces, where $G^\#$ is the right pseudoinverse of G . If the initial l_i are known to all agents and \hat{F}_{int} is constant and defined off-line, no communication is needed during task execution in order to compute G , $G^\#$.

3.2 Control

3.2.1 Feedback Linearization and Impedance Relation

We consider the inertial and geometric parameters known, so that each robot can implement a feedback linearization scheme. Setting control inputs:

$$U_i = -F_i + J_{oi}^{-T} (M_{oi}V_i + C_{oi}\dot{p}_o + G_{oi}) \quad (3.10)$$

the nonlinearities are cancelled. Auxiliary input V_i is chosen:

$$V_i = \ddot{p}_{cmd,i} + M_o^{-1}J_i^T (F_i - F_{di}) \quad (3.11)$$

and hence imposes the desired impedance behaviour

$$\ddot{p}_o = \ddot{p}_{cmd,i} + M_o^{-1}J_{oi}^T (F_i - F_{di})$$

F_{di} are the desired robot/object interaction forces:

$$F_{di} = F_{int,i} - J_{oi}^{-T}c_i (C_o\dot{p}_o + G_o + M_o\ddot{p}_{cmd,i}) \quad (3.12)$$

We choose F_{di} such that they cancel object's nonlinearities, they ensure adequate internal forces and achieve motion control. Coefficients c_i are the load distribution coefficients. They are subject to constraints:

$$\begin{aligned} c_l + c_f &= 1 \\ c_i &> 0 \end{aligned} \quad (3.13)$$

If the manipulators are heterogenous, we should assign bigger coefficient to the more capable of lifting weight. Finally, the commanded acceleration signal is responsible for the tracking objective:

$$\ddot{p}_{cmd,i} = \ddot{p}_{di} - D_i (\dot{p}_o - \dot{p}_{di}) - K_i (p_o - p_{di}) \quad (3.14)$$

Desired signal p_{dl} is the original desired trajectory profile to be implemented by the leader, while follower's desired signal p_{df} is only the estimation of the leader's. If we replace equations (3.10)-(3.11),(3.14) into the dynamic model (3.7) we obtain for both robots:

$$\Delta\ddot{p}_i + D_i\Delta\dot{p}_i + K_i\Delta p_i = M_o^{-1}J_{oi}^T (F_i - F_{di}) \quad (3.15)$$

where $\Delta p_l = p_o - p_{dl}$ and $\Delta p_f = p_o - p_{df}$ are leader's and follower's tracking errors respectively. By choosing $D_i = D$, $K_i = K$ and adding equations (3.15) for $i = l, f$ and (3.8) it follows that:

$$\Delta\ddot{\bar{p}} + D\Delta\dot{\bar{p}} + K\Delta\bar{p} = 0 \quad (3.16)$$

where $\Delta\bar{p} = p - \frac{(c_l+1)p_{dl} + (c_f+1)p_{df}}{3}$. Matrices D , K are selected diagonal with positive diagonal elements such that the above system is made asymptotically stable. With this selection $\Delta\bar{p} \rightarrow 0$ exponentially and we write:

$$p_o = \frac{(c_l + 1)p_{dl} + (c_f + 1)p_{df}}{3} + \Delta\bar{p}(\Delta\bar{p}(0), \Delta\dot{\bar{p}}(0), t) \quad (3.17)$$

Therefore, error $3\frac{p_o - p_{df}}{c_l + 1}$ exponentially converges to $p_{dl} - p_{df}$.

3.2.2 Estimation law

The estimation law is based on the last result of the previous subsection. Follower's goal is to estimate leader's desired trajectory profile. Though explicit communication is not possible, the follower robot approximates $p_{dl} - p_{df}$, by measuring $3\frac{p_o - p_{df}}{c_l + 1}$. Respectively, we approximate velocity error. However, since acceleration \ddot{p} measurement is not available, error $\ddot{p}_{dl} - \ddot{p}_{df}$ cannot be approximated in the above way. Consequently, we must design an estimator that does not use derivatives of the error and is robust to disturbances caused by acceleration. For this purpose, we sacrifice asymptotic stability and use a prescribed performance estimator, which guarantees ultimate boundedness of the position's estimation error and as a result ultimate boundedness of the overall tracking error.

For every coordinate $j \in \{1, 2, \dots, 6\}$ of the position vector the expression of prescribed performance is given, $\forall t \geq 0$, by the following inequalities:

$$-\rho_j < e_j < \rho_j$$

where $e_j = 3\frac{p_{o,j} - p_{df,j}}{c_l + 1}$ and ρ_j is the performance function with desired transient and steady-state properties (for more information refer to Appendix A or [BR10]). An estimation law that achieves this performance is:

$$\dot{p}_{df,j} = k_j \ln \left(\frac{1 + \frac{e_j}{\rho_j}}{1 - \frac{e_j}{\rho_j}} \right), \text{ for } j \in \{1, 2, \dots, 6\} \quad (3.18)$$

Integration of (3.18) yields the follower's estimate $p_{df,j}$. Differentiating (3.18) we acquire the desired acceleration signal:

$$\ddot{p}_{df,j} = \frac{2k_j}{1 - \left(\frac{e_j}{\rho_j}\right)^2} \left(\frac{\dot{e}_j}{\rho_j} \right) \quad (3.19)$$

which is bounded provided performance bounds are met. As stated in subsection 2.2.1, a good choice for function ρ_j is

$$\rho_j(t) = (\rho_{j0} - \rho_{j,\infty})e^{-st} + \rho_{j,\infty}$$

Constant s controls the convergence rate, and $\rho_{j,\infty}$ the ultimate bound. ρ_{j0} is chosen to satisfy $\rho_{j0} > e_j(0)$.

Stability Analysis

We prove that prescribed performance is achieved, and therefore, the estimation error is ultimately bounded. Since the analysis is the same regardless the position variable, from here on, we drop subscript j .

Assumption 3.1. *The initial error $e(0) = 3\frac{p_{o,j}(0) - p_{df,j}(0)}{c_l + 1}$ satisfies $e(0) < |\rho(0)|$*

Theorem 3.1. *Provided the initial configuration satisfies Assum. 3.1 and leader's desired trajectory is smooth, bounded with bounded derivatives, the estimation law (3.18) guarantees error e satisfies performance bounds: $|e(t)| < \rho(t)$, $\forall t \geq 0$.*

Proof. The analysis is similar to theorem's 2.1 proof. We define the normalized error

$$\xi = \frac{e}{\rho} \quad (3.20)$$

The estimation law (3.18) may be rewritten as function of the normalized error ξ :

$$p_{df} = k \ln \left(\frac{1 + \xi}{1 - \xi} \right)$$

Differentiating ξ with respect to time, we obtain the dynamical system:

$$\dot{\xi} = h(t, \xi) \quad (3.21)$$

We also define set $\Omega_\xi = (-1, 1)$, which is open and nonempty. Owing to Assumption 3.1 we conclude that $\xi(0) \in \Omega_\xi$. Additionally, due to smoothness of a) the system's nonlinearities, b) leader's desired trajectory, c) the exponential decrease of $\Delta\bar{p}$ and d) the proposed estimation scheme, over Ω_ξ , $h(t, \xi)$ is continuous on t and for all $\xi \in \Omega_\xi$. Therefore, the hypotheses of Theorem B.1 stated in Appendix B hold and the existence of a maximal solution $\xi(t)$ of (3.21) on a time interval $[0, \tau_{max})$ such that $\xi(t) \in \Omega_\xi, \forall t \in [0, \tau_{max})$ is ensured.

Therefore, transformed error signal

$$\varepsilon(t) = \ln \left(\frac{1 + \xi(t)}{1 - \xi(t)} \right) \quad (3.22)$$

is well defined for all $t \in [0, \tau_{max})$.

Consider now the positive definite and radially unbounded function $V = \frac{1}{2}\varepsilon^2$. Differentiating with respect to time and substituting (3.18), we obtain:

$$\begin{aligned} \dot{V} &= \frac{2\varepsilon}{(1 - \xi^2)\rho} \left(\frac{3}{c_l + 1} (\dot{p}_o - \dot{p}_{df}) + \xi\dot{\rho} \right) \\ &= \frac{2\varepsilon}{(1 - \xi^2)\rho} \left(\dot{p}_{dl} - \dot{p}_{df} + \frac{3}{c_l + 1} \Delta\bar{p}(\Delta\bar{p}(0), \Delta\dot{\bar{p}}(0), t) + \xi\dot{\rho} \right) \\ &= \frac{2\varepsilon}{(1 - \xi^2)\rho} \left(\dot{p}_{dl} - k\varepsilon + \frac{3}{c_l + 1} \Delta\bar{p}(\Delta\bar{p}(0), \Delta\dot{\bar{p}}(0), t) + \xi\dot{\rho} \right) \end{aligned} \quad (3.23)$$

Since $\Delta\bar{p}$ converges to 0, $\xi \in \Omega_\xi$ and $\dot{p}_{dl}, \dot{\rho}$ are bounded by construction we arrive at:

$$|\dot{p}_{dl} + \Delta\bar{p} + \xi\dot{\rho}| \leq \bar{U} \quad (3.24)$$

for an unknown constant \bar{U} . Moreover $\rho > 0$ Consequently, $\dot{V} < 0$ when $|\varepsilon(t)| > \frac{\bar{U}}{k}$ and subsequently:

$$|\varepsilon(t)| \leq \bar{\varepsilon} = \max \left\{ \varepsilon(0), \frac{\bar{U}}{k} \right\}, \quad (3.25)$$

for all $t \in [0, \tau_{max})$. Taking the inverse of (3.22):

$$-1 < \frac{e^{-\bar{\varepsilon}} - 1}{e^{-\bar{\varepsilon}} + 1} = \underline{\xi} \leq \xi(t) \leq \bar{\xi} = \frac{e^{\bar{\varepsilon}} - 1}{e^{\bar{\varepsilon}} + 1} < 1 \quad (3.26)$$

Therefore, $\xi \in \Omega'_\xi = [\underline{\xi}, \bar{\xi}]$, $\forall t \in [0, t_{max})$, which is a nonempty and compact subset of Ω_ξ . Hence, assuming $\tau_{max} < \infty$ and since $\Omega'_\xi \subset \Omega_\xi$, Proposition B.1 in Appendix B dictates the existence of a time instant $t' \in [0, \tau_{max})$ such that $\xi(t') \notin \Omega'_\xi$, which is a clear contradiction. Therefore, $\tau_{max} = \infty$.

As a result, all closed loop signals remain bounded and moreover $\xi(t) \in \Omega'_\xi \subset \Omega_\xi$, $\forall t \geq 0$. Finally, from (3.20) and (3.26), we conclude that:

$$-\rho(t) < \underline{\xi}\rho(t) \leq e(t) \leq \bar{\xi}\rho(t) < \rho(t)$$

for all $t \geq 0$ and consequently follower's estimation goal is achieved. \square

Corollary 3.1. *The follower's estimation error is ultimately bounded.*

Proof. From Theorem 3.1

$$|e| = \left| p_{dl} - p_{df} + \frac{3}{c_l + 1} \Delta \bar{p}(\Delta \bar{p}(0), \Delta \dot{\bar{p}}(0), t) \right| < \rho$$

, which leads us to:

$$|p_{dl} - p_{df}| < \rho + \frac{3}{c_l + 1} \Delta \bar{p}(\Delta \bar{p}(0), \Delta \dot{\bar{p}}(0), t) \quad (3.27)$$

Since $\rho \rightarrow \rho_\infty$ and $\Delta \bar{p} \rightarrow 0$ the ultimate bound is roughly ρ_∞ . \square

Corollary 3.2. *Object's trajectory tracking error is ultimately bounded.*

Proof.

$$|p_o - p_{dl}| = \left| (p_{df} - p_{dl}) \frac{c_f + 1}{3} + \Delta \bar{p} \right| < \frac{c_f + 1}{3} \rho + \frac{3}{c_l + 1} \Delta \bar{p}$$

The ultimate bound is roughly $\frac{c_f + 1}{3} \rho_\infty$. \square

Remark 3.1. *The above bounds depend directly on ρ_∞ , which can be chosen arbitrarily small. Convergence rate depends on both parameter s of ρ and the choice of matrices D, K in eq.(3.16).*

Remark 3.2. *If we are interested in velocity tracking, we can omit position terms in the commanded acceleration (3.14) and use velocity error instead of position error in (3.18). Then instead of producing a velocity reference \dot{p}_{df} we produce an acceleration reference \ddot{p}_{df} .*

Remark 3.3. *This method does use any explicit on-line communication. The only information needed on-line is sensor measurements (force, position, velocity). Some parameters, though, must explicitly be transmitted off-line, namely matrices D, K , coefficients c_i and initial positions $l_i(0)$ relative to the object. Still, this amount of information is not considerable*

Remark 3.4. *Some drawbacks of this method are the need for a common coordinate system (knowledge of inertial frame I), exact knowledge of the geometrical (lengths of links and relative positions) and inertial (M, C, G matrices) properties.*

Remark 3.5. *This method expands Kosuge's previous method, by making estimation more robust to nonzero acceleration. Furthermore, we include the object's mass in our model, which was neglected before. Finally, load distribution is implemented.*

3.2.3 Secondary Objectives

Recall from section 3.1 the decomposition of joint torque inputs:

$$\tau_i = J_i^T U_i + \left(I - J_i^T J_i^{-T} \right) \tau_{in}$$

We can use τ_{in} to achieve secondary objectives. For example, we define cost $V(q) = V_{obst} + V_{manip}$ that we want to maximize. Maximization of the cost means, the redundant DOF's are used for better obstacle avoidance and manipulability. It is reasonable to put $\tau_{in} = -k\nabla V$

3.3 Simulation

We consider a simple 1D scenario, where the leader's desired trajectory is a sinusoid and the load is equally shared. A comparison between the previous and our new method is made. We put $D = 1$, $K = 10$ and equal coefficients $c_f = c_l = 0.5$. We also suppose that the initial estimation $x_{df}(0)$ equals to $x(0)$, which is known to the follower. As depicted in figures 3.3- 3.5, the new method is more robust. Even if the error does not exactly converge to zero, it can be kept arbitrarily small. Kosuge's original method cannot converge without an acceleration estimation, which is not possible.

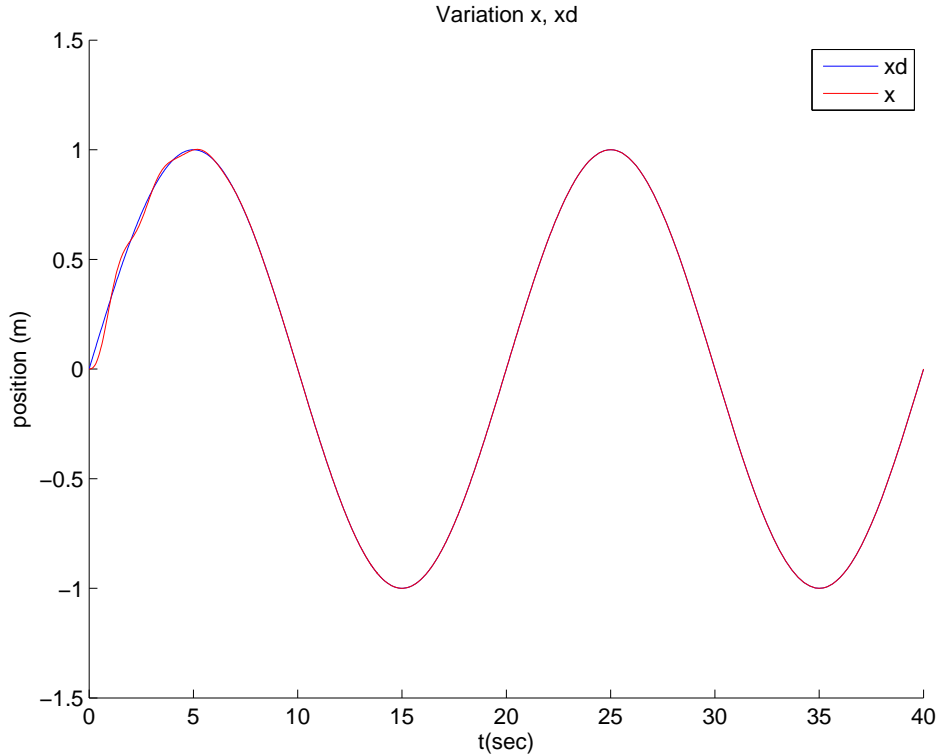


Figure 3.3: Variation

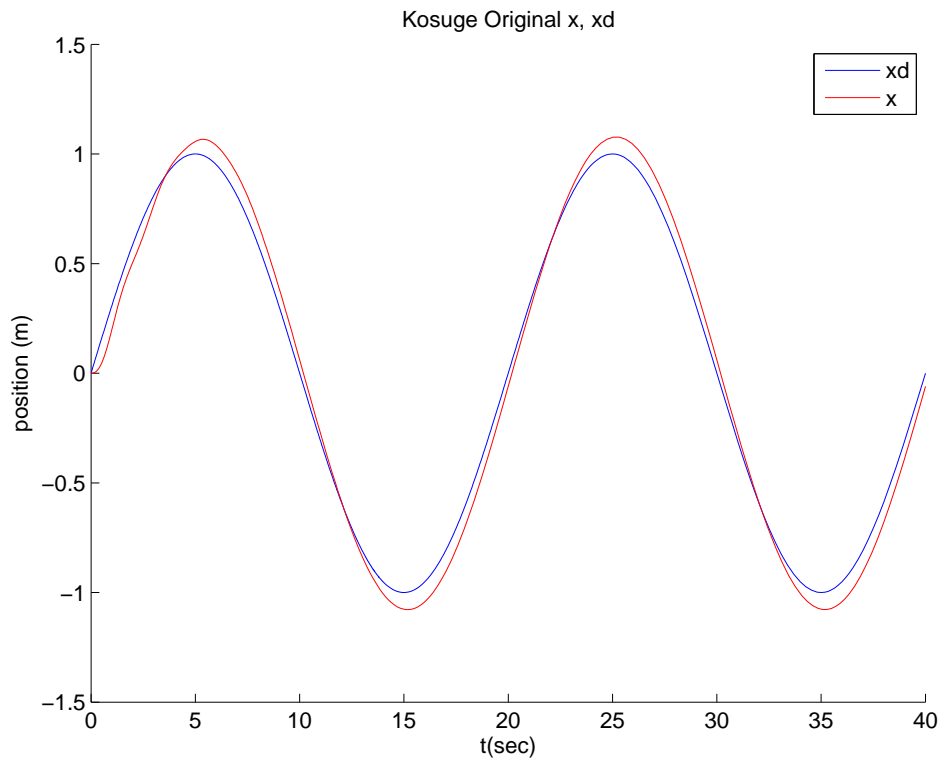


Figure 3.4: Original

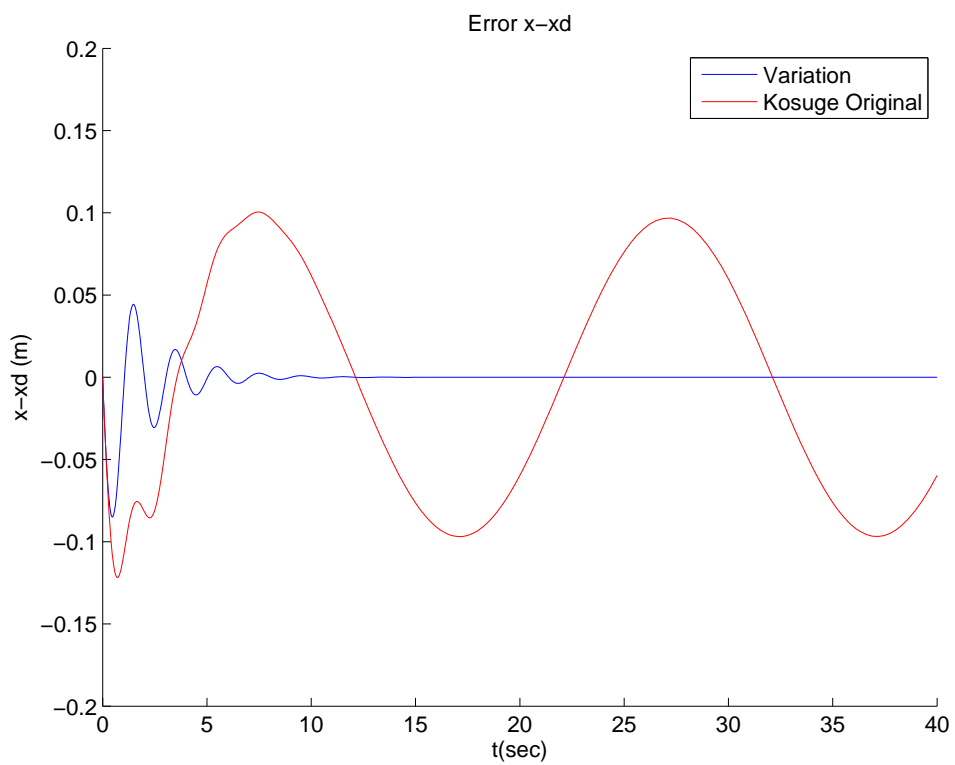


Figure 3.5: Superimposed errors

Chapter 4

Conclusion and future directions

This thesis presented two possible scenarios of cooperative manipulation under implicit communication, with their respective control schemes. We managed to completely avoid explicit on-line communication, with the only off-line information exchanged being a few parameters. We used position, velocity and force sensing, both formations were decentralized and of leader-follower architecture.

In the nonholonomic mobile robot case, we used additional revolute joints and a compliant follower-object contact to increase the mobility of the overall formation. The follower's goal to keep force constant and torque zero, resulted in keeping the contact stable and the misalignment error close to zero, as a side effect. The controller used, was based in prescribed performance methodology. With the follower's goals satisfied, the overall system was modelled as a perturbed car-like system. Depending on the availability of leader's misalignment angle sensing, we discerned two cases, the open and closed loop cases. Based on chained form representation we applied the Astolfi's control law for both cases. The robustness analysis followed by the simulations showed the superiority of the closed loop scheme.

In the holonomic mobile manipulator case, we kept the contacts rigid. The leader imposed a desired trajectory profile via an impedance relation, while the follower imposed its estimate via an impedance relation with the same constants. Due to the contacts being rigid and the impedance constants being the same, it was possible to design an estimator. We extended previous work by introducing the object's mass, implementing load sharing and making the estimation process more robust to non-zero desired acceleration.

4.1 Future directions

- Extend the point stabilization approach in subsection 2.3.3 to the trajectory tracking problem.
- Explore the possibility of employing more than one followers in the second scenario. The concept of the virtual leader presented in [KO96] could be used. However, the proof of estimator's convergence could be challenging.
- Make the scheme in chapter 3 adaptive, in order to compensate for unknown

inertial or geometric parameters.

- Effectively, use explicit communication alongside implicit to exploit the advantages of both types of communication. One possible way is to switch among different protocols depending on the situation, i.e. switch to implicit when stealth is required, switch to explicit when a collision is imminent etc. Of course, switching needs a higher level of control, which makes decisions based on some specifications. Another way is to build a set of possible movements, the execution of which needs only implicit communication. The explicit communication will be limited to a symbolic level, i.e. type of movement transmitted from the leader to the follower.

Appendices

Appendix A

Prescribed Performance

The prescribed performance notion was originally employed to design neuro-adaptive controllers, for various classes of nonlinear systems, namely feedback linearizable [BR08], strict feedback [BR09] and general MIMO affine in the control [BR10], capable of guaranteeing output tracking with prescribed performance. In this work, by prescribed performance, it is meant that the output tracking error converges to a predefined arbitrarily small residual set with convergence rate no less than a certain predefined value. This appendix summarizes preliminary knowledge on prescribed performance.

In that respect, consider a generic scalar tracking error $e(t)$. Prescribed performance is achieved if $e(t)$ evolves strictly within a predefined region that is bounded by certain functions of time. The mathematical expression of prescribed performance is given, $\forall t \geq 0$, by the following inequalities:

$$\rho_L(t) < e(t) < \rho_U(t) \quad (\text{A.1})$$

where $\rho_{L,U}(t)$ are smooth and bounded functions of time satisfying $\lim_{t \rightarrow \infty} \rho_U(t) > \lim_{t \rightarrow \infty} \rho_L(t)$, called performance functions. The aforementioned statements are clearly illustrated in Fig. A.1 for exponential performance functions $\rho_i(t) = (\rho_{i0} - \rho_{i\infty})e^{-l_i t} + \rho_{i\infty}$ with $\rho_{i0}, \rho_{i\infty}, l_i, i \in \{L, U\}$ appropriately chosen constants.

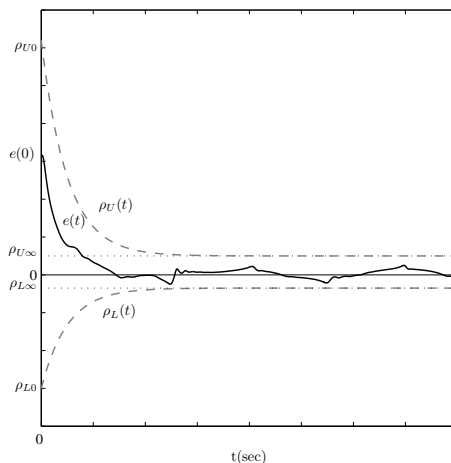


Figure A.1: Graphical illustration of the prescribed performance definition.

The constants $\rho_{L0} = \rho_L(0)$, $\rho_{U0} = \rho_U(0)$ are selected such that $\rho_{U0} > e(0) > \rho_{L0}$. The constants $\rho_{L\infty} = \lim_{t \rightarrow \infty} \rho_L(t)$, $\rho_{U\infty} = \lim_{t \rightarrow \infty} \rho_U(t)$ represent the maximum allowable size of the tracking error $e(t)$ at the steady state, which may even be set arbitrarily small to a value reflecting the resolution of the measurement device, thus achieving practical convergence of $e(t)$ to zero. Moreover, the decreasing rate of $\rho_L(t)$, $\rho_U(t)$ which is affected by the constants l_L , l_U in this case, introduces a lower bound on the required speed of convergence of $e(t)$. Therefore, the appropriate selection of the performance functions $\rho_L(t)$, $\rho_U(t)$ imposes performance characteristics on the tracking error $e(t)$.

Appendix B

Dynamical Systems

Consider the initial value problem:

$$\dot{\xi} = h(t, \xi), \quad \xi(0) = \xi^0 \in \Omega_\xi \quad (\text{B.1})$$

with $h : \mathfrak{R}_+ \times \Omega_\xi \rightarrow \mathfrak{R}^n$ where $\Omega_\xi \subset \mathfrak{R}^n$ is a non-empty open set.

Definition B.1. [Son98] *A solution $\xi(t)$ of the initial value problem (B.1) is maximal if it has no proper right extension that is also a solution of (B.1).*

As an example, consider the initial value problem $\dot{\xi} = \xi^2$, $\xi(0) = 1$, whose solution is $\xi(t) = \frac{1}{1-t}$, $\forall t \in [0, 1)$. The solution is maximal since it cannot be defined for $t > 1$. Stated otherwise, there is no proper extension of $\xi(t)$ to the right of $t = 1$ that is also a solution of the original initial value problem.

Theorem B.1. [Son98] *Consider the initial value problem (B.1). Assume that $h(t, \xi)$ is: a) locally Lipschitz on ξ for almost all $t \in \mathfrak{R}_+$, b) piecewise continuous on t for each fixed $\xi \in \Omega_\xi$ and c) locally integrable on t for each fixed $\xi \in \Omega_\xi$. Then, there exists a maximal solution $\xi(t)$ of (B.1) on the time interval $[0, \tau_{\max})$ with $\tau_{\max} > 0$ such that $\xi(t) \in \Omega_\xi, \forall t \in [0, \tau_{\max})$.*

Proposition B.1. [Son98] *Assume that the hypotheses of Theorem B.1 hold. For a maximal solution $\xi(t)$ on the time interval $[0, \tau_{\max})$ with $\tau_{\max} < \infty$ and for any compact set $\Omega'_\xi \subset \Omega_\xi$ there exists a time instant $t' \in [0, \tau_{\max})$ such that $\xi(t') \notin \Omega'_\xi$.*

Lemma B.1. (Comparison Lemma) [Kha02] *Consider the scalar differential equation*

$$\dot{u} = f(t, u), \quad u(t_o) = u_o$$

where $f(t, u)$ is continuous in t and locally Lipschitz in u , for all $t \geq 0$ and all $u \in J \subset \mathfrak{R}$. Let $[t_o, T)$ (T could be infinity) be the maximal interval of existence of the solution $u(t)$, and suppose $u(t) \in J$ for all $t \in [t_o, T)$. Let $v(t)$ be a continuous function, whose upper right-hand derivative $D^+v(t)$ satisfies the differential inequality

$$D^+v(t) \leq f(t, v(t)), \quad u(t_o) \leq u_o$$

with $u(t) \in J$ for all $t \in [t_o, T)$. Then, $v(t) \leq u(t)$ for all $t \in [t_o, T)$.

Bibliography

- [AHY⁺99] Y. Aiyama, M. Hara, T. Yabuki, J. Ota, and T. Arai. Cooperative transportation by two four-legged robots with implicit communication. *Robotics and Autonomous Systems*, 29(1):13–19, 1999.
- [AN01] M.N. Ahmadabadi and E. Nakano. A ”constrain and move” approach to distributed object manipulation. *IEEE Transactions on Robotics and Automation*, 17(2):157–172, 2001.
- [Ast95] A. Astolfi. Exponential stabilization of a car-like vehicle. In *Proceedings of the IEEE International Conference on Robotics and Automation*, volume 2, pages 1391–1396, 1995.
- [BA94] T. Balch and R. C. Arkin. Communication in reactive multiagent robotic systems. *Autonomous Robots*, 1(1):1–25, 1994.
- [BDR10] C. P. Bechlioulis, Z. Doulgeri, and G. A. Rovithakis. Neuro-adaptive force/position control with prescribed performance and guaranteed contact maintenance. *IEEE Transactions on Neural Networks*, 21(12):1857–1868, 2010.
- [BH96] R.G. Bonitz and T.C. Hsia. Internal force-based impedance control for cooperating manipulators. *IEEE Transactions on Robotics and Automation*, 12(1):78–89, 1996.
- [BJ95] R. G. Brown and J. S. Jennings. A pusher/steerer model for strongly cooperative mobile robot manipulation. In *Proceedings of the IEEE International Conference on Intelligent Robots and Systems*, volume 3, pages 562–568, 1995.
- [BR08] C. P. Bechlioulis and G. A. Rovithakis. Robust adaptive control of feedback linearizable mimo nonlinear systems with prescribed performance. *IEEE Transactions on Automatic Control*, 53(9):2090–2099, 2008.
- [BR09] C. P. Bechlioulis and G. A. Rovithakis. Adaptive control with guaranteed transient and steady state tracking error bounds for strict feedback systems. *Automatica*, 45(2):532–538, 2009.
- [BR10] C. P. Bechlioulis and G. A. Rovithakis. Prescribed performance adaptive control for multi-input multi-output affine in the control nonlinear

- systems. *IEEE Transactions on Automatic Control*, 55(5):1220–1226, 2010.
- [Bro83] R. W. Brockett. Asymptotic stability and feedback stabilization. In R. W. Brockett, R.S. Millman, and Sussmann H.H., editors, *Differential Geometric Control Theory*, pages 181–208, 1983.
- [DCJR97] W. C. Dickson, Robert H. Cannon Jr., and S. M. Rock. Decentralized object impedance controller for object/robot-team systems: Theory and experiments. In *Proceedings of the IEEE International Conference on Robotics and Automation*, volume 4, pages 3589–3596, 1997.
- [DJR97] B.R. Donald, J. Jennings, and D. Rus. Information invariants for distributed manipulation. *International Journal of Robotics Research*, 16(5):673–702, 1997.
- [Don95] B.R. Donald. On information invariants in robotics. *Artificial Intelligence*, 72(1-2):217–304, 1995.
- [GMD06] R. Groß, F. Mondada, and M. Dorigo. Transport of an object by six pre-attached robots interacting via physical links. In *Proceedings of the IEEE International Conference on Robotics and Automation*, pages 1317–1323, 2006.
- [Kha88] O. Khatib. Object manipulation in a multi-effector robot system. In *Proceedings of the 4th International Symposium on Robotics Research*, volume 4, pages 137–144. MIT Press, 1988.
- [Kha02] Hassan K. Khalil. *Nonlinear Systems*. Prentice Hall, 3rd edition, 2002.
- [KO96] K. Kosuge and T. Oosumi. Decentralized control of multiple robots handling an object. In *Proceedings of the IEEE International Conference on Intelligent Robots and Systems*, volume 1, pages 318–323, 1996.
- [KOC97] K. Kosuge, T. Oosumi, and K. Chiba. Load sharing of decentralized-controlled multiple mobile robots handling a single object. In *Proceedings of the IEEE International Conference on Robotics and Automation*, volume 4, pages 3373–3378, 1997.
- [KOS97] K. Kosuge, T. Oosumi, and H. Seki. Decentralized control of multiple manipulators handling an object in coordination based on impedance control of each arm. In *Proceedings of the IEEE International Conference on Intelligent Robots and Systems*, volume 1, pages 17–22, 1997.
- [KOS⁺98] K. Kosuge, T. Oosumi, M. Satou, K. Chiba, and K. Takeo. Transportation of a single object by two decentralized-controlled nonholonomic mobile robots. In *Proceedings of the IEEE International Conference on Robotics and Automation*, volume 4, pages 2989–2994, 1998.

- [KYC⁺96] O. Khatib, K. Yokoi, K. Chang, D. Ruspini, R. Holmberg, and A. Casal. Vehicle/arm coordination and multiple mobile manipulator decentralized cooperation. In *in proceedings of the IEEE International Conference on Intelligent Robots and Systems*, volume 2, pages 546–553, 1996.
- [LAO96] Y. H. Liu, S. Arimoto, and T. Ogasawara. Decentralized cooperation control: non-communication object handling. In *Proceedings of the IEEE International Conference on Robotics and Automation*, volume 3, pages 2414–2419, 1996.
- [LZ87] J.Y.S. Luh and Y.F. Zheng. Constrained relations between two coordinated industrial robots for motion control. *International Journal of Robotics Research*, 6(3):60–70, 1987.
- [MP10] S.A.A. Moosavian and E. Papadopoulos. Cooperative object manipulation with contact impact using multiple impedance control. *International Journal of Control, Automation and Systems*, 8(2):314–327, 2010.
- [NGB⁺09] S. Nouyan, R. Groß, M. Bonani, F. Mondada, and M. Dorigo. Teamwork in self-organized robot colonies. *IEEE Transactions on Evolutionary Computation*, 13(4):695–711, 2009.
- [PPCC02] G.A.S. Pereira, B.S. Pimentel, L. Chaimowicz, and M.F.M. Campos. Coordination of multiple mobile robots in an object carrying task using implicit communication. In *Proceedings of the IEEE International Conference on Robotics and Automation*, volume 1, pages 281–286, 2002.
- [RDJ95] D. Rus, B. Donald, and J. Jennings. Moving furniture with teams of autonomous robots. In *Proceedings of the IEEE International Conference on Intelligent Robots and Systems*, volume 1, pages 235–242, 1995.
- [SB93] D. J. Stilwell and J. S. Bay. Toward the development of a material transport system using swarms of ant-like robots. In *Proceedings of the IEEE International Conference on Robotics and Automation*, volume 1, pages 766–771, 1993.
- [SB00] D. J. Stilwell and B. E. Bishop. Framework for decentralized control of autonomous vehicles. In *Proceedings of the IEEE International Conference on Robotics and Automation*, volume 3, pages 2358–2363, 2000.
- [SCJ92] S. A. Schneider and R. H. Cannon Jr. Object impedance control for cooperative manipulation: Theory and experimental results. *IEEE Transactions on Robotics and Automation*, 8(3):383–394, 1992.
- [SK98] T. Sugar and V. Kumar. Decentralized control of cooperating mobile manipulators. In *Proceedings of the IEEE International Conference on Robotics and Automation*, volume 4, pages 2916–2921, 1998.
- [SK08] Bruno Siciliano and Oussama Khatib, editors. *Springer Handbook of Robotics*. Springer, 1st edition, 2008.

- [Son98] E. D. Sontag. *Mathematical Control Theory*. Springer, London, U.K., 1998.
- [SSVO09] Bruno Siciliano, Lorenzo Sciavicco, Luigi Villani, and Giuseppe Oriolo. *Robotics : modelling, planning and control*. Advanced Textbooks in Control and Signal Processing. Springer, 1st edition, 2009.
- [TBK04] C.P. Tang, R. Bhatt, and V. Krovi. Decentralized kinematic control of payload transport by a system of mobile manipulators. In *Proceedings of the IEEE International Conference on Robotics and Automation*, pages 2462–2467, 2004.
- [TLK03] H.G. Tanner, S.G. Loizou, and K.J. Kyriakopoulos. Nonholonomic navigation and control of cooperating mobile manipulators. *IEEE Transactions on Robotics and Automation*, 19(1):53–64, 2003.
- [YS01] S. Yamada and J. Saito. Adaptive action selection without explicit communication for multirobot box-pushing. *IEEE Transactions on Systems, Man and Cybernetics Part C: Applications and Reviews*, 31(3):398–404, 2001.